



uOttawa

L'Université canadienne  
Canada's university

FACULTÉ DES ÉTUDES SUPÉRIEURES  
ET POSTDOCTORALES



FACULTY OF GRADUATE AND  
POSTDOCTORAL STUDIES

Wei Zhang

AUTEUR DE LA THÈSE / AUTHOR OF THESIS

M.A.Sc. (Mechanical Engineering)

GRADE / DEGREE

Department of Mechanical Engineering

FACULTÉ, ÉCOLE, DÉPARTEMENT / FACULTY, SCHOOL, DEPARTMENT

Simulation and Experimental Study of Room Acoustics

TITRE DE LA THÈSE / TITLE OF THESIS

Dr. D. Neculescu

DIRECTEUR (DIRECTRICE) DE LA THÈSE / THESIS SUPERVISOR

W. Hallett

CO-DIRECTEUR (CO-DIRECTRICE) DE LA THÈSE / THESIS CO-SUPERVISOR

EXAMINATEURS (EXAMINATRICES) DE LA THÈSE / THESIS EXAMINERS

Dr. M. Liang

Dr. J. Sasiadek

Gary W. Slater

Le Doyen de la Faculté des études supérieures et postdoctorales / Dean of the Faculty of Graduate and Postdoctoral Studies

# **Simulation and Experimental Study of Room Acoustics**

By

Wei Zhang

Thesis submitted to the

Faculty of Graduate and Postdoctoral Studies

In partial fulfillment of the requirements

For the degree of Master of Applied Science

Department of Mechanical Engineering

University of Ottawa

© Wei Zhang, Ottawa, Canada, 2006



Library and  
Archives Canada

Bibliothèque et  
Archives Canada

Published Heritage  
Branch

Direction du  
Patrimoine de l'édition

395 Wellington Street  
Ottawa ON K1A 0N4  
Canada

395, rue Wellington  
Ottawa ON K1A 0N4  
Canada

*Your file* *Votre référence*  
*ISBN: 978-0-494-18484-4*  
*Our file* *Notre référence*  
*ISBN: 978-0-494-18484-4*

**NOTICE:**

The author has granted a non-exclusive license allowing Library and Archives Canada to reproduce, publish, archive, preserve, conserve, communicate to the public by telecommunication or on the Internet, loan, distribute and sell theses worldwide, for commercial or non-commercial purposes, in microform, paper, electronic and/or any other formats.

The author retains copyright ownership and moral rights in this thesis. Neither the thesis nor substantial extracts from it may be printed or otherwise reproduced without the author's permission.

**AVIS:**

L'auteur a accordé une licence non exclusive permettant à la Bibliothèque et Archives Canada de reproduire, publier, archiver, sauvegarder, conserver, transmettre au public par télécommunication ou par l'Internet, prêter, distribuer et vendre des thèses partout dans le monde, à des fins commerciales ou autres, sur support microforme, papier, électronique et/ou autres formats.

L'auteur conserve la propriété du droit d'auteur et des droits moraux qui protègent cette thèse. Ni la thèse ni des extraits substantiels de celle-ci ne doivent être imprimés ou autrement reproduits sans son autorisation.

---

In compliance with the Canadian Privacy Act some supporting forms may have been removed from this thesis.

Conformément à la loi canadienne sur la protection de la vie privée, quelques formulaires secondaires ont été enlevés de cette thèse.

While these forms may be included in the document page count, their removal does not represent any loss of content from the thesis.

Bien que ces formulaires aient inclus dans la pagination, il n'y aura aucun contenu manquant.

  
**Canada**

## **Abstract**

Sound propagation is a complex subject, especially in an enclosure. The study of room acoustics involves not only a research into how sound is propagated in a room , but also a search into how to measure sound under different condition and how to control sound in the case of various wall materials.

For an acoustical environment, there are three separated parts: sound sources, room acoustics, and the listens. These three items form a source-medium-receiver chain, which is typical for most of communication models. In this thesis, the image method is applied to predict the acoustical quality of a real room, and the experiment for room acoustic measurement is set up. The simulation model using image method proved the design of the measurement system is efficient for room acoustics.

## **Acknowledgements**

I would like to express my sincerest appreciation to Dr. Dan Neculescu, my supervisor, for offering me such an interesting research opportunity, and more importantly for his guidance, advice, patience and endless understanding throughout this research. He has been a constant source of information and support for this thesis.

I would like to thank all the staff of department of Mechanical Engineering for their various supports

Finally, I would like particularly to thank my husband Yi Lu, whose continuous support and patience throughout my research have enable me to produce this thesis.

# Contents

Abstract

Acknowledgements

Table of Contents

List of Figures

List of Table

Chapter 1	Introduction	1
1.1	Background	1
1.2	Motivation of research	2
1.3	Content of thesis	4
Chapter 2	Literature Review	5
2.1	The main room acoustics modeling principles	5
2.2	Wave-based methods	6
2.3	Ray-based methods	9
2.3.1	Ray tracing method	10
2.3.2	Image source method	10
2.4	Physical scale modeling method	11

Chapter 3	Sound processing with DAQ hardware	13
3.1	System 1 description	13
3.1.1	The amplifier	15
3.1.2	Software	16
3.1.3	Results from system 1	18
3.2	System 2 description	19
Chapter 4	Room acoustics modeling	27
4.1	Wave equation for an enclosure	27
4.2	Normal modes and eigenfrequencies of a rectangular room	29
4.3	FEMLAB calculation of room eigenvalue and acoustics pressure distribution	36
Chapter 5	Simulation study of room acoustics	45
5.1	Image method	45
5.2	Simulation model	50
5.3	Simulation results	59
Chapter 6	Experimental study of the room acoustics	70
6.1	Sound card	70
6.2	The experimental setup	74
Chapter 7	Conclusion and recommendation for future work	83

7.1	Conclusion	83
7.2	Future work	84
	References	86
	Appendix	90
	Simulation codes	90

## List of Figures

2.1	Room acoustics modeling methods	6
2.2	Finite element grids for a room	7
3.1	The diagram of system 1	13
3.2	Circuit diagram of inverting amplifier	14
3.3	Pin layouts for LM741 operational amplifier	15
3.4	Block diagram in Labview	16
3.5	The front panel (cut off frequency of 2000Hz)	17
3.6	The front panel (cut off frequency of 1000Hz)	18
3.7	The diagram of xPC system	20
3.8	The Simulink model	20
3.9	The input signals in xPC system	21
3.10	The input signals spectrum	21
3.11	The low pass antialiasing filter	22
3.12	The output signals after passing through the low pass filter with cut off frequency of 2000Hz	23
3.13	The spectrum of the output signals after passing through the low pass filter with cut off of frequency 2000Hz	23
3.14	The output signals after passing through the low pass filter with cut off frequency of 1000Hz	24
3.15	The spectrum of the output signals after passing through the low pass filter with cut off of frequency 1000Hz	24

3.16	The output signals after passing through the low pass filter with cut off frequency of 500Hz	25
3.17	The spectrum of the output signals after passing through the low pass filter with cut off of frequency 500Hz	25
4.1	Dimensions of a rectangular room	28
4.2	Eigenfrequencies –space for a rectangular room	32
4.3	Resonance mode	34
4.4	Resonance mode	34
4.5	Simulated room	36
4.6	FEMLAB windows setting for calculation 55 eigenvalues up to $1e4$	38
4.7	The mesh for the simulation room	38
4.8	The pressure distribution for the eigenvalue, $7.19e2$ (4.3Hz)	39
4.9	The pressure distribution for the eigenvalue, $3.4e3$ (9.3Hz)	40
4.10	The pressure distribution for the eigenvalue, $9,9e3$ (15.8Hz)	40
4.11	The pressure distribution for the eigenvalue, $2.58e4$ (12.8Hz)	41
4.12	The pressure distribution for the eigenvalue, $3.4e3$	42
4.13	The pressure distribution for the eigenvalue, $2.5e5$	43
5.1	Reflection of the light ray	45
5.2	The reflection of a beam of the light on a smooth hard wall	47
5.3	Spherical waves from a point source and are reflected by a hard wall	48
5.4	A source with one level images	50
5.5	Reflection paths with two levels of images	50
5.6	Reflection path involving three levels of images	51

5.7	A sound source with different levels of images	52
5.8	The simulation model	52
5.9	Image sources in a rectangular room	54
5.10	The flow chart of Matlab program	59
5.11	Reflection diagrams for the room with rigid surfaces	60
5.12	Schematical diagram for the room with nonrigid surfaces	60
5.13	Frequency spectrum for one cycle of the sine wave $x = \sin 200\pi t$	61
5.14	Receiver signal for one cycle of the sine wave $x = \sin 200\pi t$ for a room with rigid walls	62
5.15	The reflection diagram for one cycle of the sine wave $x = \sin 200\pi t$ in the case of nonrigid walls	62
5.16	Frequency spectrum for one cycle of the sine wave $x = \sin 2000\pi t$	63
5.17	The reflection diagram for the sine wave $x = \sin 2000\pi t$ for nonrigid walls	64
5.18	The reflection diagram for the sine wave $x = \sin 2000\pi t$ for nonrigid walls	64
5.19	The sound signals for the input	65
5.20	The frequencies of the input signals	66
5.21	Response for the room with rigid walls	66
5.22	Response for the room with nonrigid walls	67
5.23	The impulse response in the anechoic room	68
6.1	Scheme for the digital processing of an analog signal	70
6.2	The pulse signal	70

6.3	The individual impulse function with evenly time period	72
6.4	The analog input signal	72
6.5	The sampled input signal	73
6.6	Experimental setup for room acoustics measurement	74
6.7	The input signals	75
6.8	Frequency-domain representation of the input signals	76
6.9	Experimental outputs of the signals from the microphone	76
6.10	Frequency-domain representation of the output signals	77
6.11	Simulation results at the microphone location	77
6.12	The output signals from the microphone with the significant noise	78
6.13	The frequency distribution of the output signals	79
6.14	The frequency of the output signals after passing through the low pass filter with cut-off frequency 1500Hz	79
6.15	The output signals after passing through the low pass filter with the cut-off frequency 1500Hz	80
6.16	Simulation results for the results shown in Fig. 5-15	80

# List of Table

4.1	The frequencies distribution of the normal modes	35
-----	--	----

# Chapter 1

## Introduction

### 1.1 Background

Acoustics is the science of sound, which studies sound generation, transmission, reception and effects. The sound wave is a longitudinal mechanical wave because the velocity of the air that carries the sound moves back and forth is parallel to the direction of wave motion. A sound wave is a series of alternate increases and decreases of the air pressure. The human ear is sensitive to sound in the frequency range of 20Hz to 20KHz. The modern acoustics has broadened to frequencies too low (infrasound) or too high (ultrasound) to be heard by a person, also regarded as sound. The sound isn't restricted to the airborne vibrational waves [1]. It is extended to include similar vibrations in other gaseous, liquid, or solid media.

In an engineering sense, acoustics is divided into several areas of application, such as environmental, architectural, and atmospheric acoustics. Architectural acoustics are concerned with the design of buildings and rooms and the use of sound absorption materials and abatement techniques [2].

Room acoustics deals with sound propagation in enclosures. In room acoustics, only the air is the transmission medium in room acoustics. How sound emanates from a source

depends on a sound field, which is the region surrounding the source. It includes the room size and geometry and the combined effects of walls reflection, diffraction and absorption [3]. If a free field is concerned, the sound wave from a source can be spherical, and the intensity can be approximated by the inverse square law. There is no reflection of the sound wave. In a room having considerably absorbent surface, where the direct sound from the sound source predominates everywhere. This room is called an anechoic chamber or dead room. If the room surfaces are highly reflective, the intensity of the indirect sound can exceed the intensity of the direct sound. Such a room is an echoic chamber or live room, which can render a weak sound more audible. If the musical sound gets more significant reflections, this can blur the distinction between individual notes and, consequently, the listener can't hear the sound clearly. Normally the sound is heard as a combination of a direct sound, straight from a source/sources, and indirect sound, reflected by the surfaces and by objects in the room.

## **1.2 Motivation of research**

Room acoustics involves not only the behavior of sound in the room but also the design of room according to the type of activity taking place in this room. In order to understand the sound field in an enclosure, it is necessary to investigate how the sound that has lower or higher frequencies propagates in an enclosure. The difference between them is related to the room size. For example, consider a listening room that has large dimensions compared to the 3.4 wavelength of 100Hz sound. Then, below 100Hz the acoustics at different locations are dominated by several discrete resonance frequencies. Above 100Hz,

these resonance frequencies are packed so tight that the room acoustic behaviors quite uniform and it can be described by reverberations. There are two different approaches to describe the acoustical environment mentioned above [4].

When the wavelength of the sound is larger than the room dimensions, the sound field can be described by the normal modes or resonances, which are the three dimensional standing waves. Each mode is associated with an eigenfrequency. There is a different sound pressure distribution corresponding to each eigenfrequency. The frequency of resonance is higher in small rooms due to the smaller dimensions and shorter wavelengths. For this reason, standing waves are a much more important consideration in small rooms, where the frequency of interest lies within the normal speech range of 100 Hz to 5 kHz. Standing waves can cause the unnatural boosting and accentuation of certain frequency in the certain locations. Standing waves usually occur between hard parallel wall surfaces, where the sound is reflected several times back and forth between the parallel surfaces. This creates areas of differing sound pressure and the sound field is not uniform.

If the room dimensions are larger than the wavelength of the sound, the geometrical acoustics is applied to build the acoustics modeling in the room. The geometrical acoustics employs the geometrical optical techniques that replace the sound waves by the sound rays. The sound ray radiates from the source and reflects from the surfaces of the room and generates a reverberant field.

For an acoustical environment, there are three part separated parts: sound sources, room acoustics, and the listeners. These three items form a source-medium-receiver chain, which is typical for most of communication models. In this thesis the image method is applied to predict the acoustical quality of a real room, and the experimental study is used to validate the simulation results.

### **1.3 Content of thesis**

This thesis is organized as follows:

**Chapter 1**, a general introduction to the thesis.

**Chapter 2**, an overview of room acoustical modeling techniques.

**Chapter 3**, two systems are set up using the data acquisition (DAQ) systems to acquire the acoustic signals with a microphone.

**Chapter 4** analyses a sound field in a room, characterized by the normal mode using analytical method and finite element method using FEMLAB. The various spatial distributions of acoustic pressure for different eigenfrequencies calculated using FEMLAB.

**Chapter 5** presents the image source method in detail. The simulation model and results are presented.

**Chapter 6** presents the experimental setup, in order to characterize the acoustical environment to measure the sound efficiently in a real room.

**Chapter 7** concludes the thesis and presents suggestions for future work.

## **Chapter 2**

### **Literature Review**

It is always difficult for the researcher in architectural acoustics to predict the sound quality accurately in an enclosure when they design a concert or conference hall. The sound propagation is a complex subject and there are numerous papers and books that present different types of methods. However, it is impossible to achieve an absolutely accurate description of the sound propagation in a real room. Each method has some limitations [5]. In this section, we will introduce several methods commonly used for acoustic modeling in the room acoustics.

#### **2.1 The Main Room Acoustics Modeling Principles**

There are three different approaches for room acoustics modeling, which are discussed in this paper, are showed in Fig. 2-1. Physically the description of sound propagation in an enclosed space is based on the wave equation, known also in the form of Helmholtz equation. Theoretically, a source-to-receiver impulse response can be obtained by solving the wave equation, but it can be applied only for a simple case. The reason is that the sound propagation is complicated in the practical situations, such for the acoustical characterization of a room that has irregular shape. Instead, it is convenient to employ the sound ray to replace the sound wave. These are called ray-based methods that are based on

geometrical room acoustics. Besides these two methods, the physical scale modeling method is also introduced.

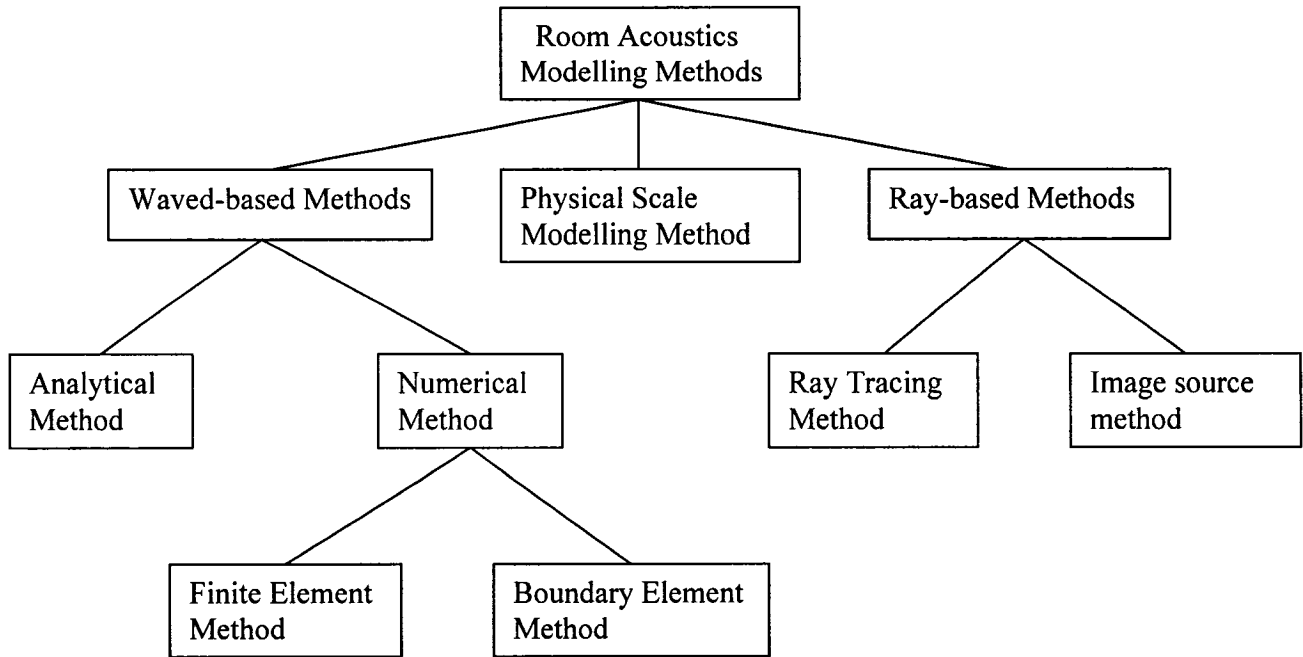


Figure 2-1 Room acoustics modeling methods

## 2.2 Wave-based Methods

Wave-based methods are based on the general solution of the wave equation. One of wave-based method is the analytical solution method. In analytical method the boundary conditions along the surfaces have to be set up and the solution of the wave equation must satisfy these boundary conditions. An example using the analytical method is discussed in Chapter 4.

The commonly used method is the numerical method [6] [7]. The numerical solution methods divide the models into small elements that can be accurately represented by the wave equation. Therefore, a complex enclosure can be expressed by a number of small elements that have a simple geometry. The numerical methods like finite element method (FEM) or boundary element method (BEM) are currently suitable only for small rooms and low frequencies due to the limitation in numerical computation with digital computers [8][9].

Fig. 2-2 [10] shows acoustic finite element grids for a room. The more complex the room geometry is, the larger the number of elements needed. Also the number of the elements depends on the frequency range of the sound. The elements must have the dimensions that are smaller than half a wavelength in order to satisfy the requirements of the sampling theorem.

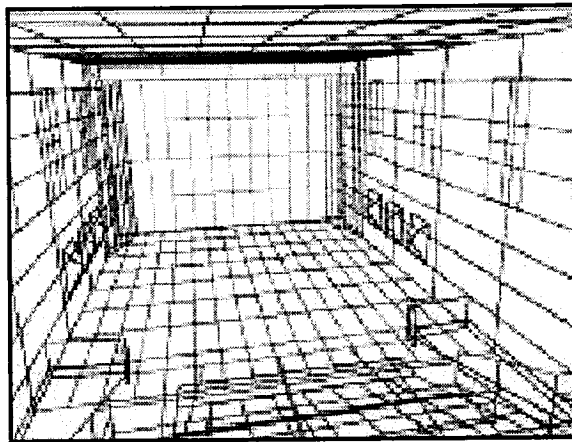


Figure 2-2 Finite element grids for a room

There are a variety of ways to divide a given enclosure. Rectangular elements are most often used. When the enclosure is divided into elements, there are many intersection

points called nodes. With a larger number of nodes, the results would be more accurate, but the heavy numerical computation is required due to the greater number of integration points needed and the complex input data.

A main limitation of FEM is that the whole space has to be modeled. This is also the fundamental difference between FEM and BEM [7]. In FEM, the complete space needs to be discretized. Instead, in BEM the boundaries of space are discretised. Consequently the major advantage of BEM over FEM is that only the boundary surfaces are modeled as a mesh of elements. As a result, the matrices are large and sparse in FEM, whereas the matrices used in BEM are small and dense.

With these element methods, it is convenient to create a denser mesh, required no matter where the location is, such as the corners of the room, which have an important influence on the sound propagation. Another benefit of the element methods is that it is easy to make coupled models.

The wave equation provides the most accurate results. But its application is limited by the lack of detailed knowledge on the definition of the boundary conditions. For example, it is hard to find the data in existing literature regarding the complex impedance for various situations [5].

### **2.3 Ray-based Methods**

The ray-based methods are based on geometrical room acoustics in which the sound wave is assumed represented by a sound ray. The assumption is permitted when the dimension of the room and the surfaces are large compared to the wavelength of sound.

There are two commonly used ray-based methods that give an approximate solution for the sound propagation in an enclosure. One is the ray tracing method [11][12] and the other is the image method [13][14][15]. The basic distinction between these two methods is the way the reflection paths are calculated. In the ray tracing technique, only a finite number of sound rays are constructed from the source to the receiver. Some valid ray paths may not be included in the calculated results [16] [17]. Using the ray tracing method, the simulation results can be obtained for a complex geometry. The image method can find all sound ray paths but, the computation time increases rapidly with higher order of reflection in the simulation and as a result only early reflections are computed. The maximum achieved order of reflections depends on the room geometry and computation capability, while higher order reflections can be calculated with the ray tracing method. The hybrid ray-tracing method / image source method is also used. It results in a slightly increased computation time to take advantage of the ray tracing method, and also achieves the accuracy of the image source method [18].

### **2.3.1 Ray tracing method**

The ray tracing method is an algorithm of the geometrical presentation of the sound propagation in an acoustic space [11][12][16][17][19]. There are various ways to implement the ray tracing method. The basic algorithm is that the sound rays from the sound source move with the sound speed and are subject to the laws of geometric acoustics; the listener receives rays from audible reflections. For acoustic studies, the sound rays are emitted in either the randomized way or the predefined way [11]. The ray tracing method assumes to have a uniform distribution of rays over a sphere and obtains a statistic result.

In the ray tracing method the listener is modeled as volumetric objects, such as spheres and cubes, but the listener may also be assumed as planar. In theory, a listener can be of any shape if there are enough rays to arrive to the listener for achieving statistically valid results. A sphere is the best choice in most cases, because it provides an omnidirectional sensitivity pattern and it is easy to implement.

### **2.3.2 Image source method**

Image source method is one of the fundamental ray-based methods [13][14][15][20][21][22]. It has much in common with the ray tracing method, but instead of tracing a limited selection of initial rays, the image source method can calculate all ray paths from all possible combinations from reflecting walls. Allen and Berkley proposed an efficient algorithm for the image method for a rectangular room [13]. The algorithm is presented in detail in chapter 5.

The most serious problem of the image method is that a long computer time is required because of the very high number of image sources needed.

## **2.4 Physical scale modeling method**

The physical scale modeling method has been applied in the room acoustics since 1930s [5] [23]. The principle of the physical scale modeling method is based on similarity theory. In this method a real, three dimensional scale model of the space is constructed. Apart from the air absorption, all of the acoustic aspects of this scale model are almost the

same as its prototype at full size. For a 10:1 scale model, the dimension of the scale model is tenth of dimension of the full size space. Thus the frequency range is up to ten times higher than that in full size and all of the acoustic effects remain in proportion.

The physical scale modeling method requires measurement equipment capable of measuring ultrasonic signals and signal acquisition equipment. For example, the small loudspeakers must deliver a power output similar to that of real loudspeakers and to provide a reasonable signal-noise ratio. As a result of advancement of instrumentation, the physical scale modeling is now well proven and reliable. The advantage of the method is a more correct simulation of reflections with complex geometry if diffraction, diffusion and edge reflections are important. Also, the listener test may be performed on the scale model [24].

The main limitation of the scale models is that air absorption is more difficult to model [5][25][26]. Nitrogen and dry air may be the better way to model the behavior of real air at a scale model, but this is expensive. The important aspects of the material for the scale models such as absorption coefficients, reflection and diffraction properties are another problem. Even though these can be measured, the results of the measurement depend on the way of the measurement is carried out and the acoustic environment. There are no guaranties that the physical properties of the material scale are chosen correctly and this limits the application of the physical scale modeling method.

## **Chapter 3**

### **Sound processing with DAQ hardware**

The data acquisition (DAQ) systems are extensively applied in a wide range of laboratory applications. A DAQ system usually consists of sensors, signal conditioning, plug-in DAQ board, and software for acquiring the signal from the sensors. In order to analyze the frequencies of the sound, two systems built to acquire the acoustic signal with a microphone are presented in this chapter.

#### **3.1 System 1**

This system 1 setup is used to acquire the signals through a microphone from human voice and to send the signals to the analog input of the DAQ hardware. Then, applying Labview software, the signals are stored and filtered. The filtered signals are sent to an analog output of the DAQ board and transmitted to a speaker to hear the processed sound. Fig.3-1 shows the diagram of this system.

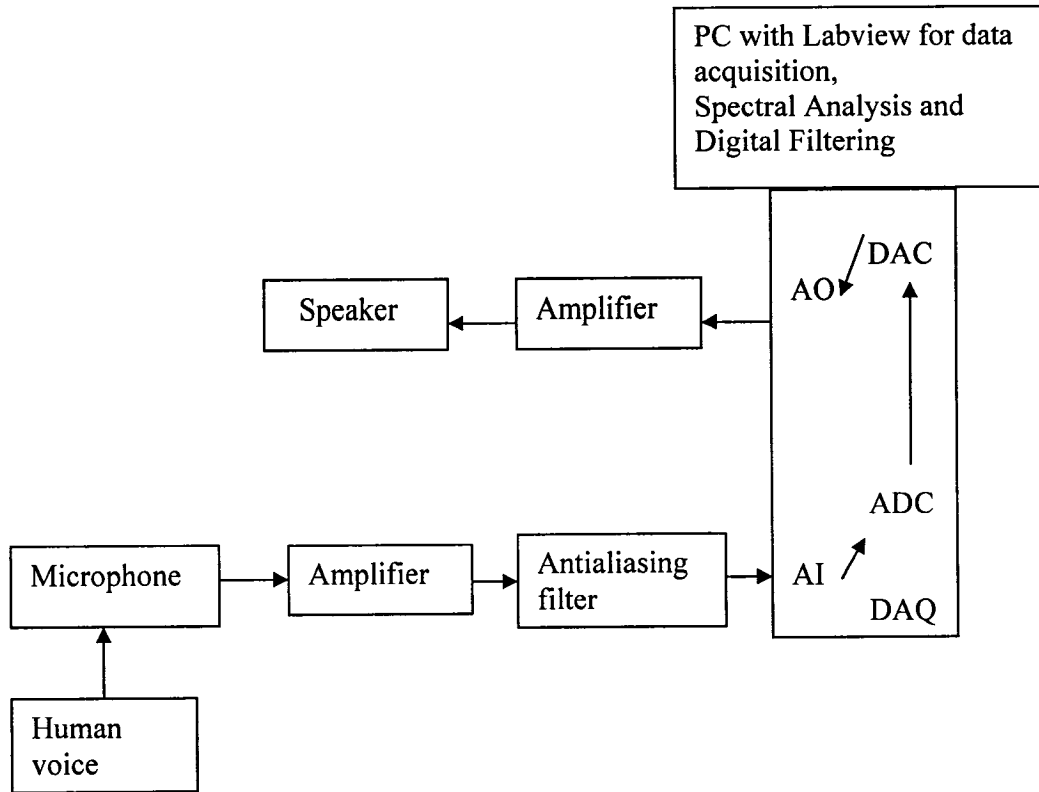


Figure 3-1 The diagram of the first system 1

A microphone is a transducer, i.e. a device that changes sound information from one form, which exists as patterns of air pressure, to another form, as patterns of electric current. Normally, microphone outputs are very weak electric signals. These low-level signals need to be conditioned to a level that DAQ board can read.

### 3.1.1 The amplifier

Microwave signal was amplified using an inverting operational amplifier. The following hardware has been used in building the inverting amplifier circuit shown in the Fig.3-2, consisting of.

- 1)  $1\text{K}\Omega$  and  $100\text{K}\Omega$  resistors.
- 2) LM741 (operation amplifier)
- 3) 2 power supplier 9V DC sources
- 4) Breadboard

The LM741 amplifier, shown in the Fig. 3-3, uses five terminals (pins 2, 3, 4, 6, 7). Two terminals are used for input purposes and are designed as (-) and (+) input terminals 2 and 3. Two other terminals are used for the dc supplies while the fifth one (numbered as 6 in the pin diagram) is for the output. The amplifier is powered by DC source, connected at pins 7 and 4.

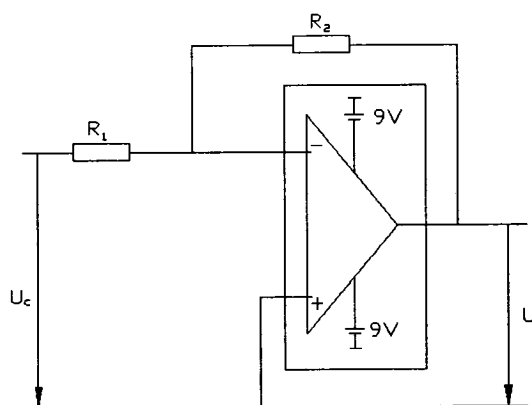


Figure 3-2 Circuit diagram of inverting amplifier

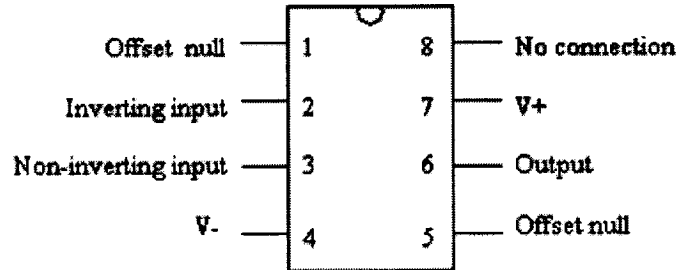


Figure 3-3 Pin layouts for LM741 operational amplifier

The output generated from microphone is in mil volts. This low voltage is amplified using the above presented inverting operational amplifier with a gain of 100. The output of the amplifier is around 2 volts, which is compatible DAQ board AI. The output of the inverting operational amplifier is determined by the ratio of the feedback resistor ( $R_2$ ) to the input resistor ( $R_1$ ).

$$U = -(R_2 / R_1)U_c$$

Gain of 100 was achieved by choosing the value of  $R_1 = 1K\Omega$  and  $R_2 = 100K\Omega$ .

### 3.1.2 Software

In order to acquire the signals from the microphone, a Labview VI is programmed. This VI can be found in “Data acquisition”> “analog input”> “AI Acquire Waveform.vi. Because the normal voice speaking ranges from 100 to 3500Hz, the sampling rate must be at least twice the maximum frequency to avoid aliasing, in accordance to Nyquist’s theorem. Channel 4 was specified with a sampling rate of 10000 and the number of sample was also

chosen as 10000. After receiving the signals, VIs for digital filtering and spectrum analysis, were included.

In spectrum analysis, the time domain is transformed to the frequency domain. FFT.VI was used to do this operation, as shown in Fig.3-4.

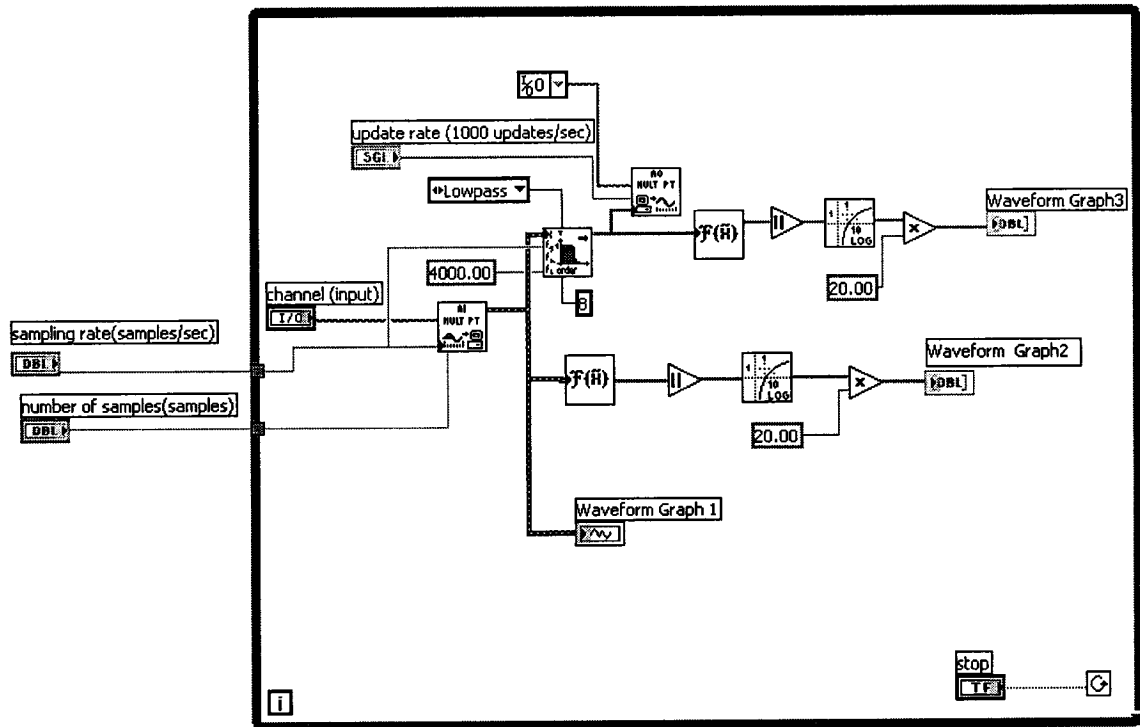


Figure 3-4. Block diagram in Labview

The VIs from Labview used for this purpose and shown in Fig 3.4 are:

1. “AI MULT PI” for acquiring the signal from “channel (input)” at given “sampling rate” for the “number of samples”.
2. A “low pass” filter is shown in Fig.3-4, in this case for 4000Hz cut off frequency.
3. F (H) spectrum is shown the frequencies of the signal.

### 3.1.3 Results from system 1

In a first set of results the low pass filter with the cut off frequency 2000Hz was used, followed by the spectrum analysis. The results are shown in Fig.3-5. For the cut off frequencies of 1000Hz and, the spectrum analysis, the results are showed in Fig. 3-6. In Fig. 3-5 and Fig. 3-6 the graph 1 and graph 2 show the amplitude vs. time of the input and the amplitude vs. frequency of the input. The graph 3, the amplitude vs. frequency shows the effect of the low pass filter. These effects are less obvious in graph 1, the amplitude vs. time and this justifies frequency analysis. Graph 2, amplitude vs. frequency of the input signal can be used as a reference for the analysis of the filtered results.

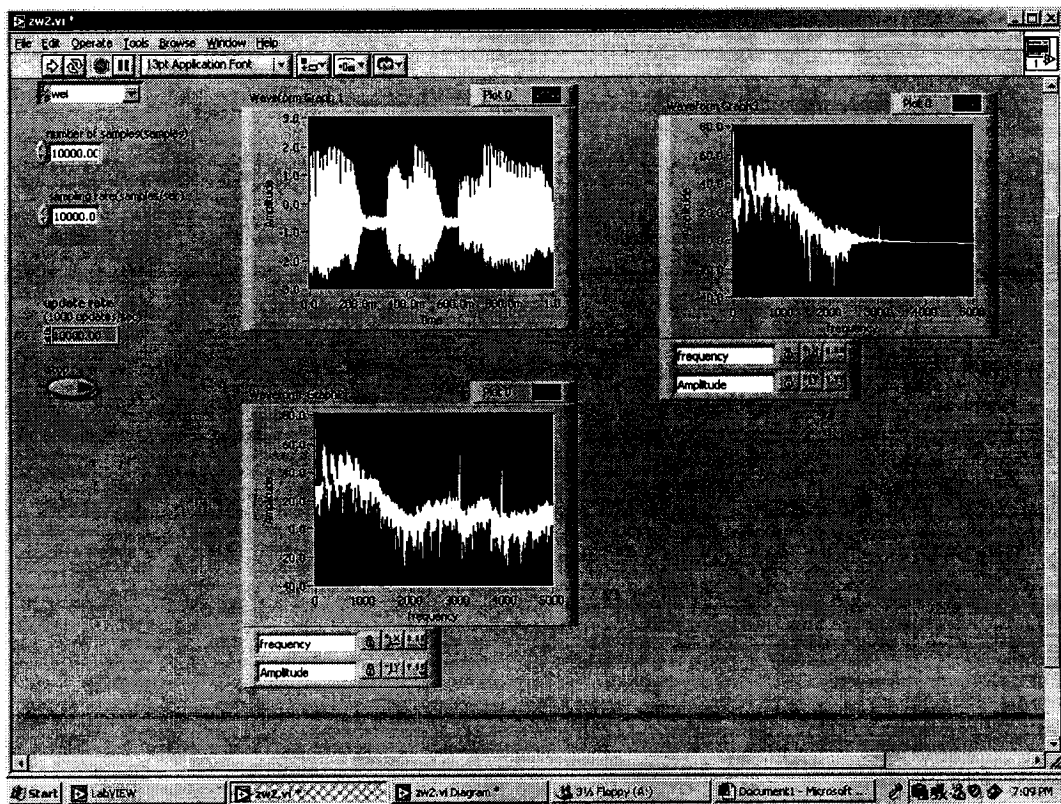


Figure 3-5 The front panel (cut off frequency of 2000Hz)

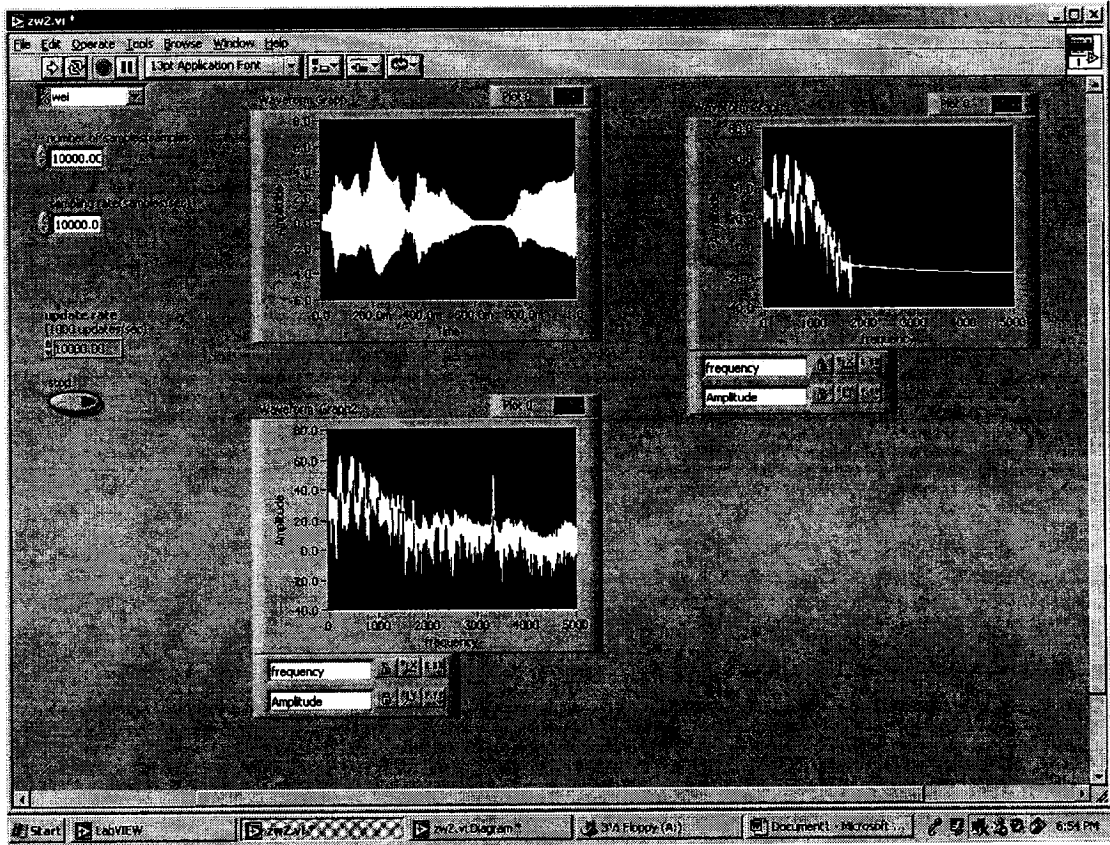


Figure 3-6 The front panel (cut off frequency of 1000Hz)

When the signals pass through low pass filter, the sound from the speaker is weaker than the original sound because the low pass filter remove the sound whose frequencies are higher than 1000Hz. Labview program permits to hear the voice from the speaker when we speak to the microphone, but the problem was that the sound we heard delayed about one second, and this defeats the purpose of real time application. For this reason an xPC Target was used to achieve real time performance.

## 3.2 System 2

xPC Target is a product from The Math Works, a host-target PC solution for prototyping, testing, and deploying real-time systems. A desktop PC was used as a host computer with MATLAB, Simulink, and Real-Time Workshop to create models using Simulink blocks, run simulations, and generates code. A second desktop PC was used as a target computer, where the generated code runs in real time. Fig.3-7 shows the diagram of the xPC system. The microphone is connected to the microphone input of the sound card. A cable is connected from the line output of the sound card to the analog input of DAQ board. Fig.3-8 shows Simulink model. The I/O driver blocks are added to the simulink model. The analog output of DAQ is connected to the amplifier and the speakers. Fig. 3-8 shows the Simulink model. The signal from the "Analog input" of the PCI-6024E NI board are sent to the FFT, the analog output for the amplifier and the speakers, and to a scope. The resulting signals are shown in Fig.3-9 and Fig. 3-10, the sound input is shown in Fig. 3-9, amplitude vs. time from the microphone and in Fig. 3-10 the input spectrum. The sound input has very low amplitude noise.

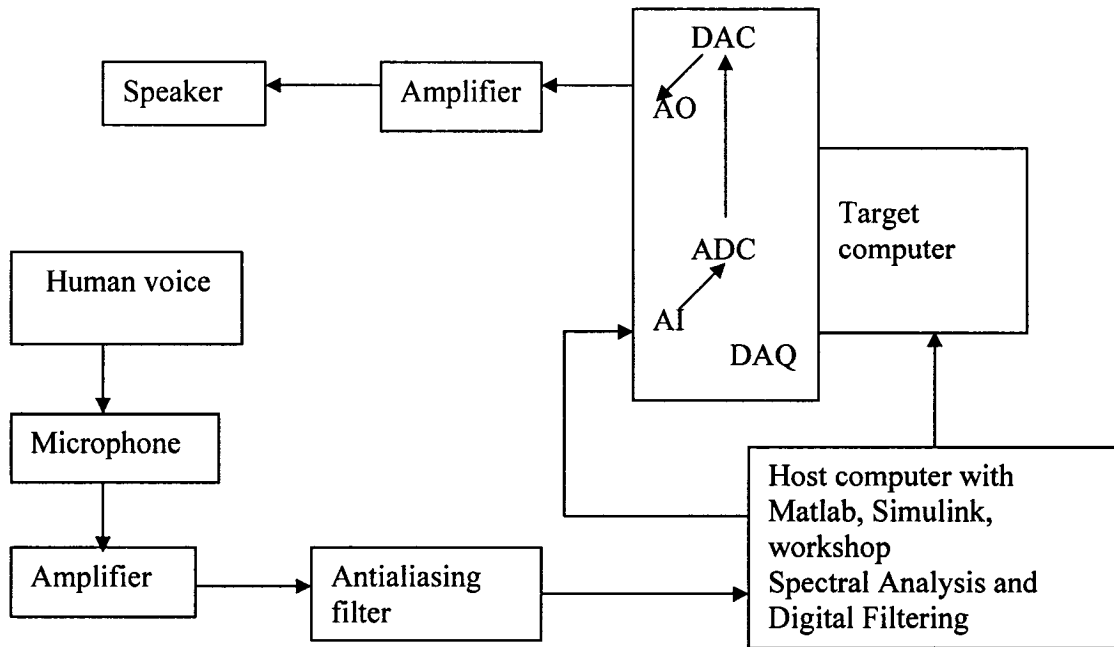


Figure 3-7 The diagram of xPC system

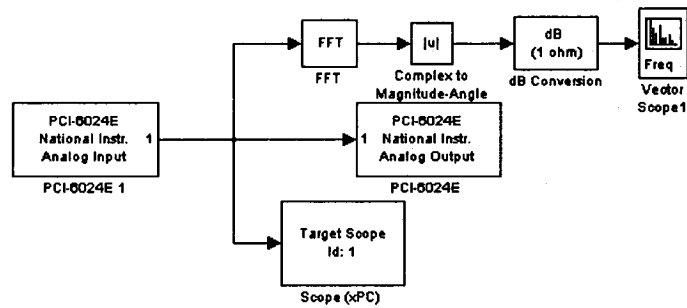


Figure 3-8 The Simulink model

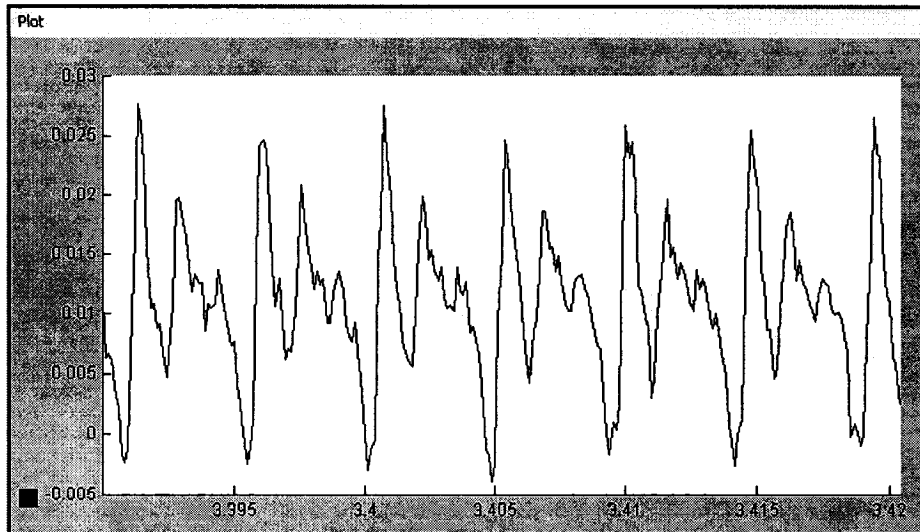


Figure 3-9 The input signals in xPC system

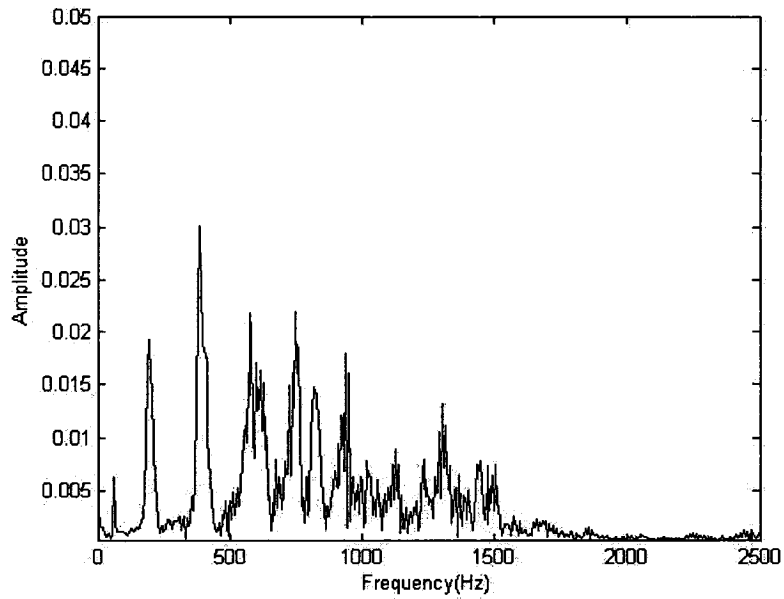


Figure 3-10 The input signals spectrum

Since normally the noise has high frequency. A low pass analog filter has to apply.

Fig.3-11 is the low pass antialiasing filter.

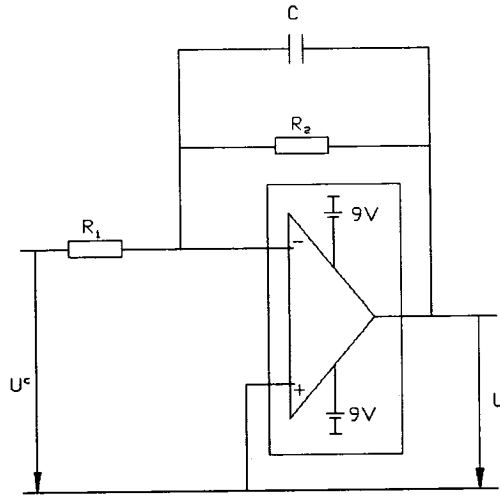


Fig.3-11 The low pass antialiasing filter.

Fig.3-12 (amplitude vs. time) and Fig.3-13 present the signals passed through a low pass filter with cut-off frequency of 2000Hz. The sound from the speaker is not significantly different from the sound because the signals have low amplitude noise. When the sound goes through the low pass filter with cut off frequency 1000Hz, shown in Fig.3-14 (amplitude vs. time) and Fig.3-15, the sound from the speakers is weaker than the input to the microphone due to removal of high frequencies of sound. Fig.3-16(amplitude vs. time) and Fig.3-17 show the signals go through the low pass filter with cut-off frequency 500 Hz. The sound heard from the speaker is very weak compared to input to the microphone, because the low pass filter removes most of high frequencies of the sound. With xPC target, the output from the speakers is practically produced in real time. PC system achieves efficiently the required signal processing.

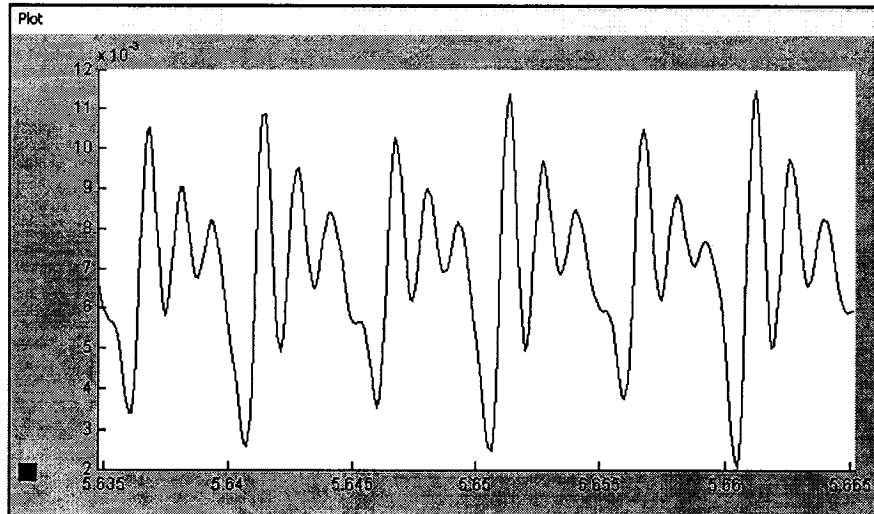


Figure 3-12 The output signals after passing through the low pass filter with cut off frequency of 2000Hz

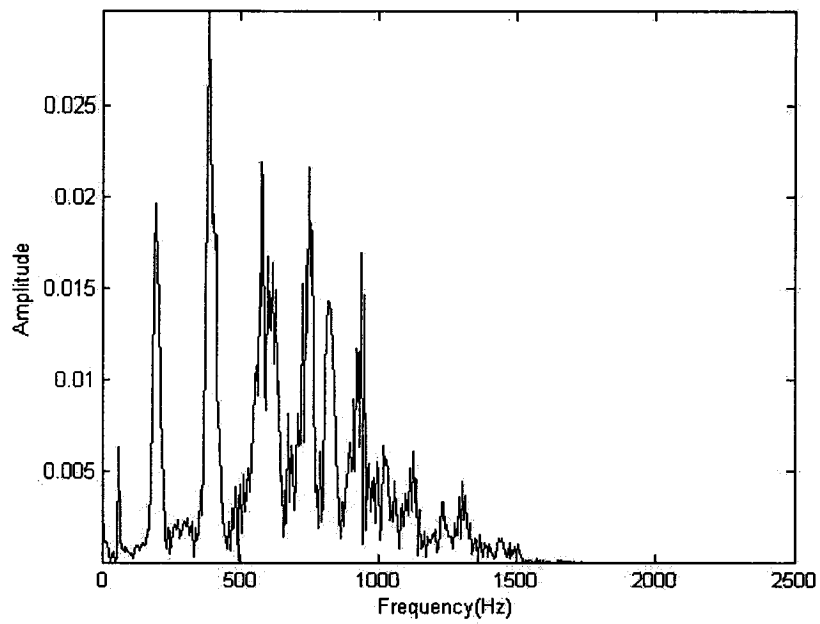


Figure 3-13 The spectrum of the output signals after passing through the low pass filter with cut off of frequency 2000Hz

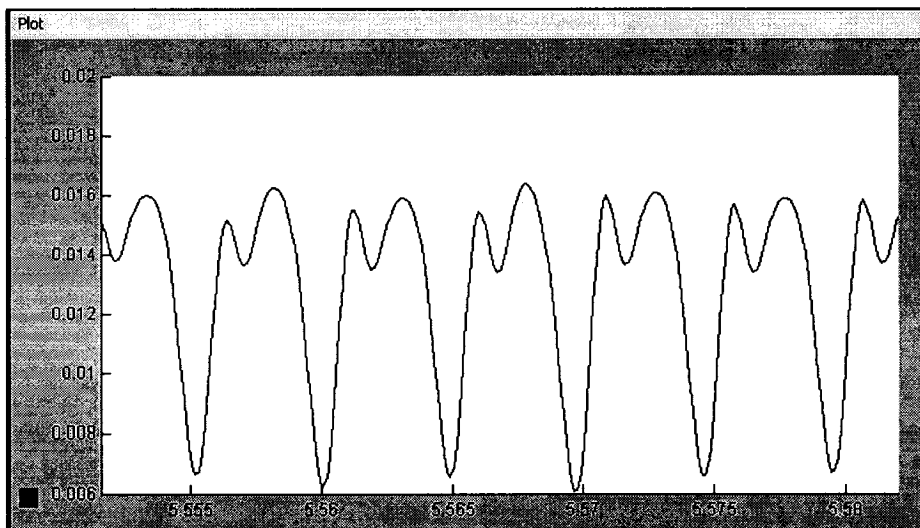


Figure 3-14 The output signals after passing through the low pass filter with cut off frequency of 1000Hz

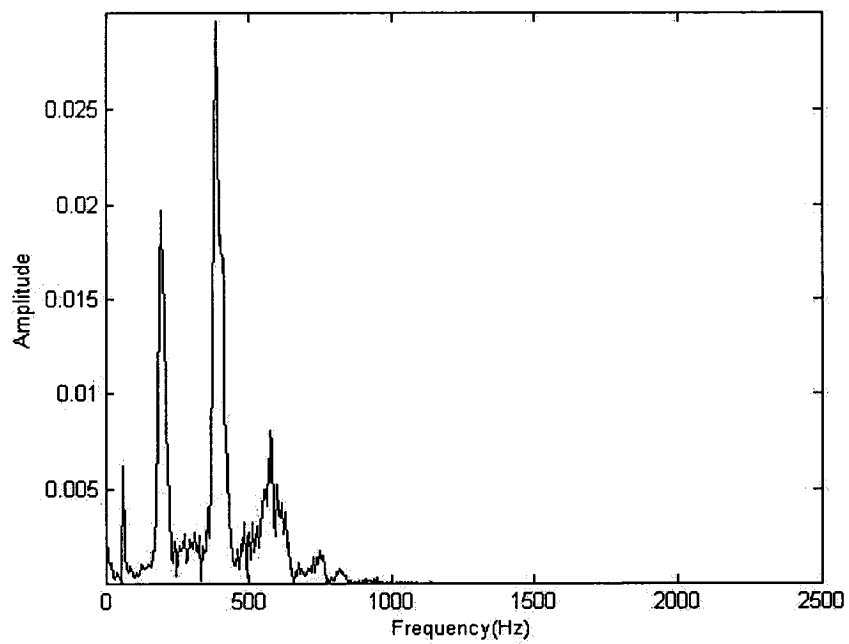


Figure 3-15 The output signals after passing through the low pass filter with cut off frequency of 1000Hz

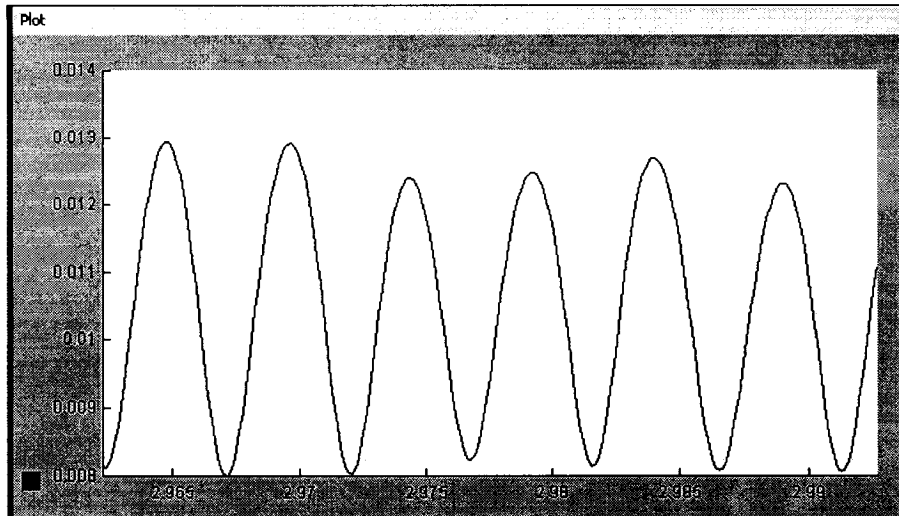


Figure 3-16 The output signals after passing through the low pass filter with cut off frequency of 500Hz

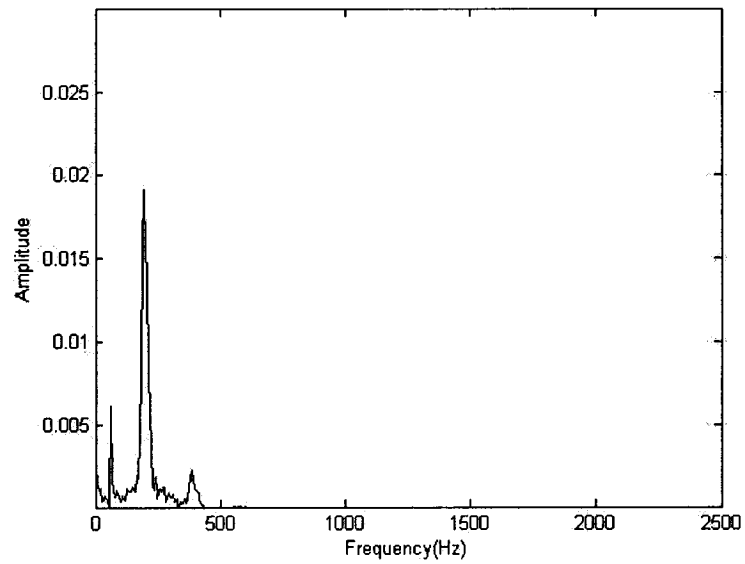


Figure 3-17 The spectrum of the output signals after passing through the low pass filter with cut off of frequency 500Hz

## Chapter 4

### Room Acoustics Modeling

The sound field in the case of low frequency can be described in precise mathematical terms. This chapter presents the acoustic wave equation and its solution. Results from FEMLAB software using the finite element method are also presented.

#### 4.1 Wave Equation for an Enclosure

The sound field can be represented by the wave equation in case of assuming a harmonic-time law for the pressure field [4] [27]. The 3D wave equation is

$$c^2 \Delta p = \frac{\partial^2 p}{\partial t^2} \quad (4-1)$$

Where, harmonic-time assumption gives

$$p(x, y, z, t) = P(x, y, z)e^{j\omega t}$$

The following equations result

$$\frac{\partial^2 p(x, y, z, t)}{\partial t^2} = -\omega^2 P(x, y, z, t)e^{j\omega t}$$

and

$$\Delta p(x, y, z) = e^{j\omega t} \Delta P(x, y, z)$$

which give

$$c^2 e^{j\omega t} P(x, y, z) = -\omega^2 \Delta P(x, y, z) e^{j\omega t}$$

The spatial wave equation for  $P(x, y, z)$  is

$$\Delta P + k^2 P = 0 \quad (4-2)$$

where  $k = \frac{\omega}{c}$

The velocity  $v_n$ , normal to the wall surface, is

$$v_n = \frac{i}{\omega \rho_0} \frac{\partial p}{\partial n} \quad (4-3)$$

where  $\frac{\partial}{\partial n}$  is a differentiation in the direction of the outward normal to the wall.

The boundary condition is based on the wall impedance  $z$ .

$$z = \frac{P}{v_n} \quad (4-4)$$

Hence the boundary condition is

$$z \frac{\partial p}{\partial n} + i\omega \rho_0 P = 0 \quad (4-5)$$

According to the wave theory, it is sufficient to obtain a solution for the acoustic field with the wave equation and the boundary condition [28].

## 4.2 Normal Modes and Eigenfrequencies of a Rectangular room

Even though the wave equation can in principle be solved for given boundary condition, it is difficult to obtain the solution for the arbitrary geometry and complex boundary condition. Since the solution of the wave equation is to illustrate certain important properties of the sound field. We limit our attention to a rectangular room with rigid surfaces. Though there is no exactly rectangular empty room in practice, most of rooms are much closer to a rectangle than any other of simple geometry [4][29].

A rectangular room bounded by three pairs of parallel planes, perpendicular to each other and to the axis of a Cartesian coordinate system, is shown in Fig.4-1.

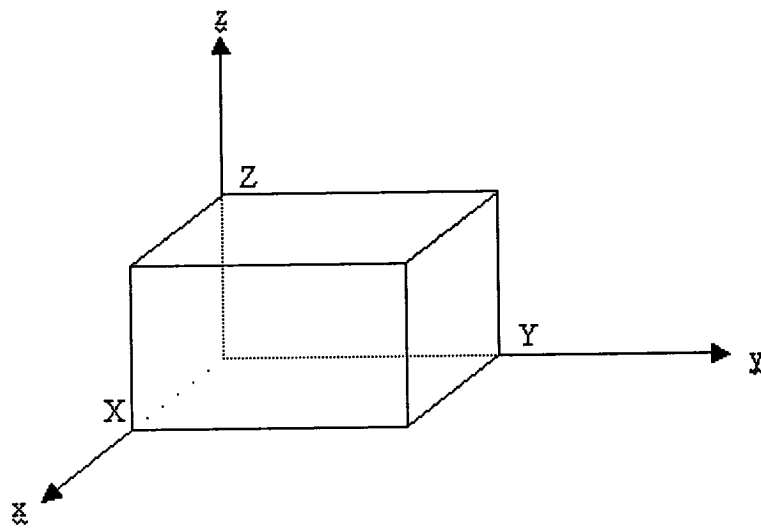


Figure 4-1 Dimensions of a rectangular room

If there is no source, homogenous spatial wave equation is

$$\frac{\partial^2 P}{\partial x^2} + \frac{\partial^2 P}{\partial y^2} + \frac{\partial^2 P}{\partial z^2} + k^2 P = 0$$

where the spatial variables can be separated as follows,

$$P(x, y, z) = P_x(x)P_y(y)P_z(z)$$

The wave equation becomes

$$\frac{\partial^2 P_x(x)}{P_x(x)\partial x^2} + \frac{\partial^2 P_y(y)}{P_y(y)\partial y^2} + \frac{\partial^2 P_z(z)}{P_z(z)\partial z^2} + k^2 = 0 \quad (4-6)$$

The first three terms depend on  $x$  only, on  $y$  only and on  $z$  only, respectively. Each of the first three terms must be constant. In this case

$$k^2 = k_x^2 + k_y^2 + k_z^2 \quad (4-7)$$

and this results in three differential equations

$$\begin{aligned} \frac{\partial^2 P_x}{\partial x^2} + k_x^2 P_x &= 0 \\ \frac{\partial^2 P_y}{\partial y^2} + k_y^2 P_y &= 0 \\ \frac{\partial^2 P_z}{\partial z^2} + k_z^2 P_z &= 0 \end{aligned} \quad (4-8)$$

We assume that the rectangular room of dimension is  $X, Y, Z$  and with rigid walls.

The boundary conditions in this case are

$$\begin{aligned} \frac{\partial p}{\partial x} &= 0 \quad \text{for } x = 0, \quad x = X \\ \frac{\partial p}{\partial y} &= 0 \quad \text{for } y = 0, \quad y = Y \\ \frac{\partial p}{\partial z} &= 0 \quad \text{for } z = 0, \quad z = Z \end{aligned}$$

The general solution of the spatial wave equation

$$P_x(x) = A_1 \cos(k_x x) + B_1 \sin(k_x x) \quad (4-9)$$

with the boundary condition

$$\frac{\partial P_x(x)}{\partial x} = -A_1 k_x \sin(k_x x) + B_1 k_x \cos(k_x x) = 0$$

In case of  $x = 0$ , the boundary condition is satisfied for  $B_1 = 0$ .

For  $x = X$ , we must have  $\sin(k_x X) = 0$  and, this is true for

$$k_x X = n\pi$$

$$k_x = \frac{n\pi}{X}$$

where  $n$  is a non-negative integer number.

Similarly, for the other two boundary conditions

$$k_y = \frac{m\pi}{Y}$$

$$k_z = \frac{l\pi}{Z}$$

where  $m, l$  are also non-negative integers.

That gives

$$k_{nml} = [(k_x^2 + k_y^2 + k_z^2)]^{1/2} = \pi[(n/X)^2 + (m/Y)^2 + (l/Z)^2]^{1/2} \quad (4-10)$$

The eigenfrequencies are given by

$$f_{nml} = \frac{kc}{2\pi} = \frac{c}{2} [(n/X)^2 + (m/Y)^2 + (l/Z)^2]^{1/2} \quad (4-11)$$

$$f_{nml}^2 = f_x^2 + f_y^2 + f_z^2 \quad (4-12)$$

and the pressure modes are given by

$$P_{nml} = A_{nml} \cos\left(\frac{n\pi}{X} x\right) \cos\left(\frac{m\pi}{Y} y\right) \cos\left(\frac{l\pi}{Z} z\right) \quad (4-13)$$

where  $A_{nml}$  is an arbitrary constant.

Using Euler equation

$$\cos x = (e^{jx} + e^{-jx})/2 \quad (4-14)$$

the pressure can be written

$$P_{nml} = \frac{A_{nml}}{8} \sum e^{\pm j\pi \frac{n}{X}x} e^{\pm j\pi \frac{m}{Y}y} e^{\pm j\pi \frac{l}{Z}z} \quad (4-15)$$

The direction of a plane wave propagation is defined by the angles  $\theta_x, \theta_y, \theta_z$

$$\cos \theta_x : \cos \theta_y : \cos \theta_z = (\pm \frac{n}{X}) : (\pm \frac{m}{Y}) : (\pm \frac{l}{Z}) \quad (4-16)$$

It means there are three different modes for the wave propagation. If one of the three constants ( $n, m, l$ ) is zero, the corresponding angle is  $90^\circ$ . The plane traveling wave is parallel to the coordinate plane of the two other axes. This kind of wave mode is called ‘tangential mode’. If there are two of the constants that are zero. The wave propagation is parallel to the axe which the corresponding constant isn’t zero. This mode is referred to as ‘axial mode’. If three of constants are all non-zero, the propagation is oblique to all three axes. This mode is called ‘oblique mode’.

With equation (4-11) and (4-12) the number of the mode for a given frequency range can be calculated. We can build a Cartesian coordinate system with axes  $f_x, f_y, f_z$ , shown in Fig. 4-2. Every normal mode is a point in a Cartesian coordinate system. The coordinate of the point is  $nc/2X, mc/2Y, lc/2Z$ . The distance from the point to the origin is  $f_{nml}$ . A point of the Cartesian coordinate system presents the frequency of a normal mode. The points indicate the number of normal mode for this frequency. Every interval along  $f_x, f_y, f_z$  axes is separately  $c/2X, c/2Y, c/2Z$ . The normal modes below 100Hz are in a sphere that has a

radius of 100Hz. Because  $f_x, f_y, f_z$  are positive, the normal mode is in a quadrant of the sphere. Every normal mode has a volume  $((c/2X) \times (c/2Y) \times (c/2Z) = c^3/8V)$  in this space.

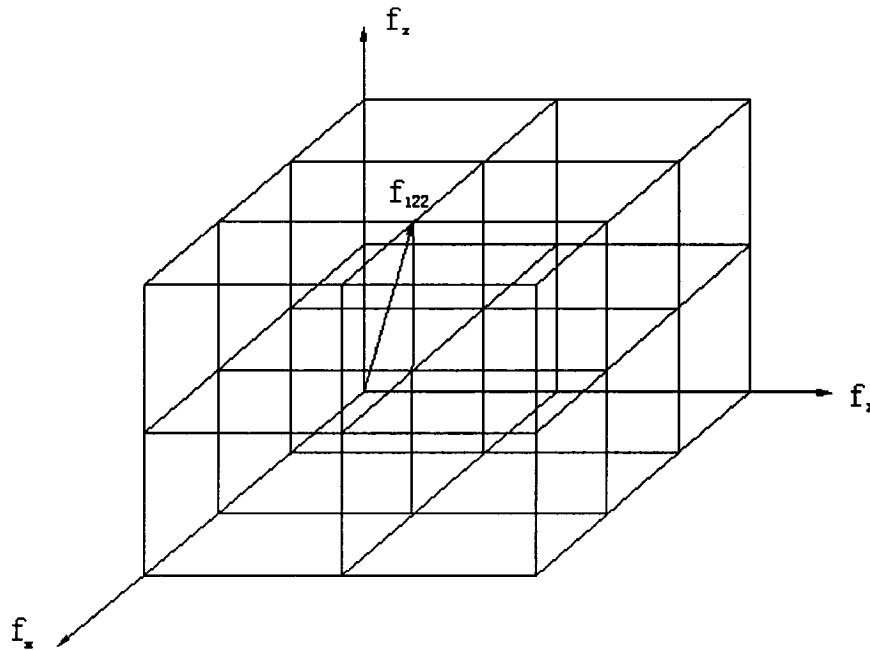


Figure 4-2 Eigenfrequencies –space for a rectangular room

The equation of calculating the number of normal modes within the frequency from 0 to an upper limit  $f$  is approximated by [4]

$$N_0 = \frac{1}{8} \cdot \frac{\pi f^2}{4} \cdot \frac{c^3}{8V} = \frac{4\pi V}{3c^3} f^3$$

However the points aren't evenly distributed in the quadrant. Some normal modes are axial ones and some are tangential modes.

The number of oblique normal modes is given by

$$N_{obl} = \frac{4\pi V}{3c^3} f^3 - \frac{\pi S}{4c^2} f^2 + \frac{L}{8c} f$$

The number of tangential normal modes is given by

$$N_{\text{tan}} = \frac{\pi S}{2c^2} f^2 - \frac{L}{2c} f$$

The number of axial normal modes is given by

$$N_a = \frac{L}{2c} f$$

The total number of the eigenfrequencies is

$$N(f) = N_{\text{obl}} + N_{\text{tan}} + N_a = \frac{4\pi V}{3c^3} f^3 + \frac{\pi S}{4c^2} f^2 + \frac{L}{8c} f$$

where

V is the volume of the room,  $V = XYZ$

S is the area of its boundary,  $S = 2(XY + XZ + YZ)$

L is the sum of the lengths of all edges of the room.  $L = 4(X + Y + Z)$

When a room is excited by the sound source at an eigenfrequency or resonance frequency, the standing waves occur [30] [31]. Some of them reinforce each other while others are cancelled. As a result, there are antinodes, where the pressure is maximum and nodes, where the pressure is zero. Fig. 4-3 shows the fundamental axial mode between two parallel walls whose distance is L. The frequency of the resonance mode is  $f = \frac{c}{2L}$ , where c is the speed of sound in the air. There are many other resonance modes whose frequencies are multiples of the fundamental mode frequency. Fig. 4-4 shows the second lowest resonance mode. The resonance modes are created, whenever the distance between the walls equals the multiples of half a wavelength. The phenomenon of standing waves happens not only between two parallel surfaces (axial modes), but also between four surfaces (tangential modes) or all six surfaces (oblique modes).

If the sound source is located at an antinode of a normal mode, the mode can be fully excited. In contrast, if the source is located at a node of the mode, the mode won't be excited no matter how loud the sound source is. Any of normal modes can be excited when the source is placed in corners of a room.

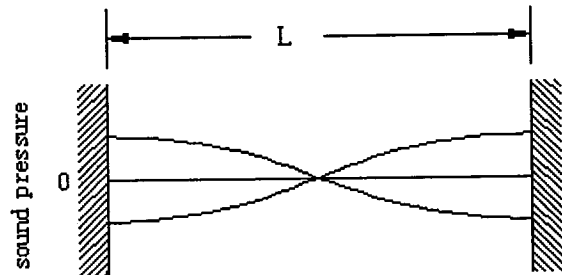


Figure 4-3 resonance mode

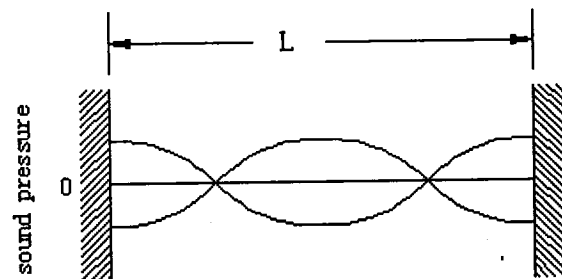


Figure 4-4 resonance mode

There is another phenomenon called 'degenerate' normal modes when two or more modes have same eigenfrequencies. It results in some areas that have much more sound loudness. Changing the room dimension can solve this situation [31] [32]. Table 4-1 shows that data for rooms, which have almost same volumes. For room 1#, the dimension ratio is

1:1:1 and the room has 16 normal modes under 100Hz, but only five different frequencies. If the room dimension rate is 1/q: 1: q, for example q is equal to  $\sqrt{2}$  for room 2#. There are 16 normal modes that include 12 different modes. For room 3# the dimension rate is 1/6:1/5:1/4 and there are 16 different normal modes.

Room 1# $V = 4.24m \times 4.24m \times 4.24m$				Room 2# $V = 3m \times 4.24m \times 6m$				Room 3# $V = 3.44m \times 4.3m \times 5.16m$			
$n$	$m$	$l$	$f_{nml}$	$n$	$m$	$l$	$f_{nml}$	$n$	$m$	$l$	$f_{nml}$
0	0	1	40.5	0	0	1	28.6	0	0	1	33.3
0	1	0		0	1	0	40.5	0	1	0	40
1	0	0		0	1	1	49.6	1	0	0	49.9
0	1	1	57.3	1	0	0	57.2	0	1	1	52
1	1	0		0	0	2	63.9	1	0	1	60
1	0	1		1	0	1	70.1	1	1	0	64
1	1	1	70.1	1	1	0	70.1	0	0	2	66.6
2	0	0	81	0	1	2	81	1	1	1	72.1
0	2	0		1	1	1	75.7	0	1	2	77.7
0	0	2		0	2	0	81	0	2	0	80
1	0	2	90.6	1	0	2	85.9	1	0	2	83.2
2	0	1		0	2	1	85.9	0	2	1	86.6
0	1	2		0	0	3	90.4	1	1	2	92.3
1	2	0		1	1	2	90.4	1	2	0	94.2
2	1	0		0	1	3	94.5	2	0	0	99.8
2	1	0		0	2	2	99.2	1	2	1	100
0	2	1									

Table 4-1 The frequencies distribution of the normal modes

### 4.3 FEMLAB calculation of room eigenvalue and acoustics pressure distribution

FEMLAB is a simulation software for modeling and solving models for phenomena that can be described with partial differential equation [43][44]. FEMLAB permits to predict how the model will function without having to build a prototype.

For the calculation of the resonance modes, we use FEMLAB's graphical interface for creating geometries, generating meshes, post-processing and visualization. The simulated room, shown in Fig. 4-5, has the dimensions  $X= 40.23$  [m],  $Y= 13.41$  [m] and  $Z = 20.70$  [m] correspond to Solomon Temple and Sixtine Chapel and contains a stage with the dimension 10 by 5 by 1 meters.

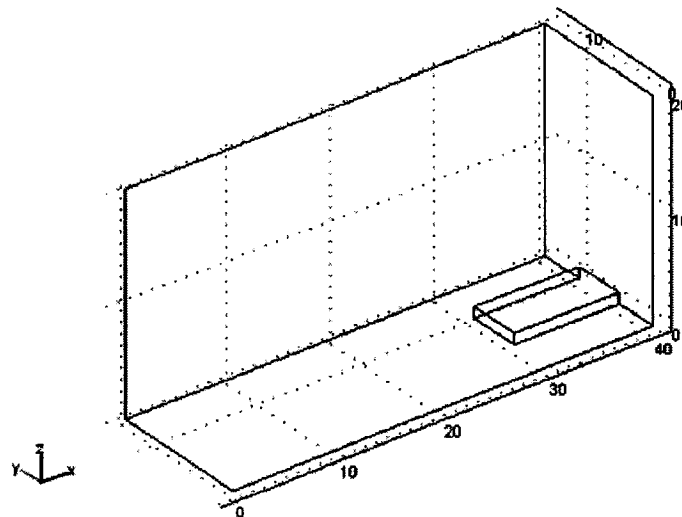


Figure 4-5 Simulated room

The modal frequencies  $f_{nml}$  [Hz] of the empty room with hard walls, in case of sound speed in air  $c = 343.6$  [m/s], or  $c/2=171.8$ , are given by

$$f_{nml} = 171.8 \sqrt{(n/40.23)^2 + (m/13.41)^2 + (l/20.70)^2} \quad \text{for } n, m, l = 0, 1, 2, 3, \dots$$

such that the eigenvalues are

$$\lambda_{nml} = \omega_{nml}^2 = 343.6^2 \pi^2 [(n/40.23)^2 + (m/13.41)^2 + (l/20.7)^2] \quad \text{for } n, m, l = 0, 1, 2, 3, \dots$$

Calculating the number of normal mode under 30Hz, according to the equations presented before, we can get

$$N_{obl} = 31$$

$$N_{tan} = 19$$

$$N_a = 3$$

The sum of the number

$$N(f) = N_{obl} + N_{tan} + N_a = 53$$

The eigenvalue for 30Hz is

$$\lambda_{30} = (\omega_{30})^2 = (2\pi f_{30})^2 = 0.355 \times 10^5 [\text{rad}^2 / \text{s}^2]$$

FEMLAB window setting for hard boundary conditions, for sound propagation in the room for 55 eigenvalues up to around  $1e5$  [ $\text{rad}^2/\text{s}^2$ ], is shown in Fig.4-6

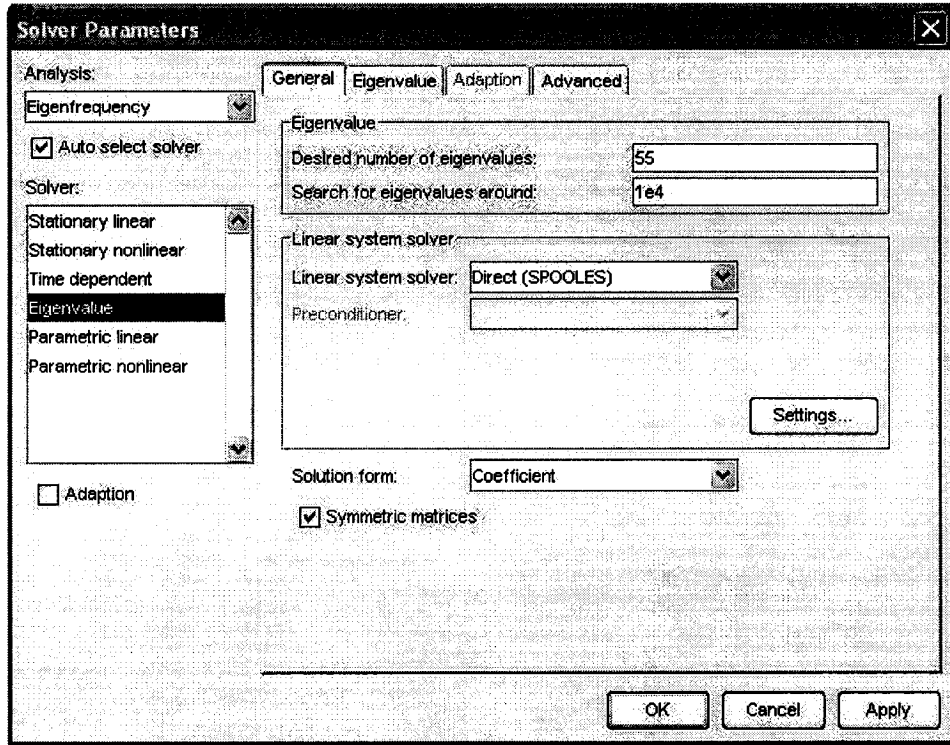


Figure 4-6 FEMLAB windows setting for calculating 55 eigenvalues up to 1e4

FEMLAB has a mesh menu to generate the meshes for the model. Figure 4-7 shows the mesh for 3-D simulation room.

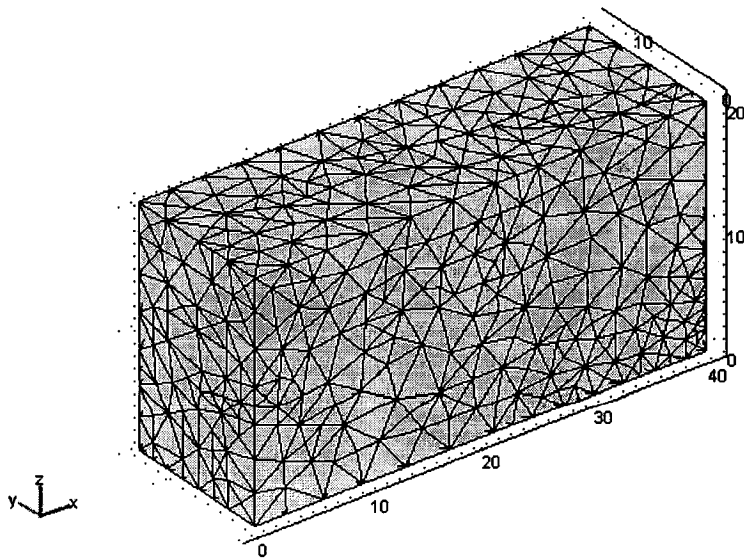


Figure 4-7 The mesh for the simulation room

Besides eigenvalues, FEMLAB permits to visualize 3-D pressure distribution for the simulation room. Figure 4.8-4.10 show the pressure distribution for the boundary plot of three modes: mode (1,0,0), mode (1,0,1), mode (1,1,1). Different colors indicate the different pressures and the brighter the colors, the higher the pressure is. From these graphs, the number  $n, m, l$  in a mode means the number of planes of zero pressure occurring along the  $x, y, z$  coordinates, respectively.

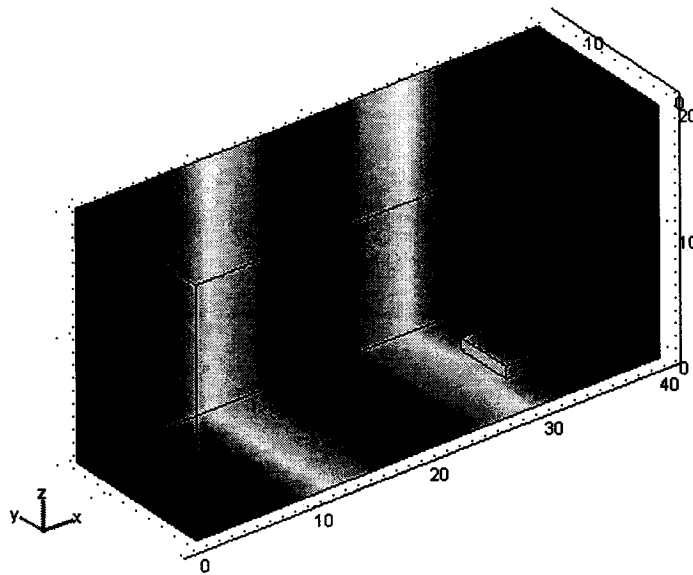


Figure 4-8 The pressure distribution for the eigenvalue,  $7.19e2$  (4.3Hz)

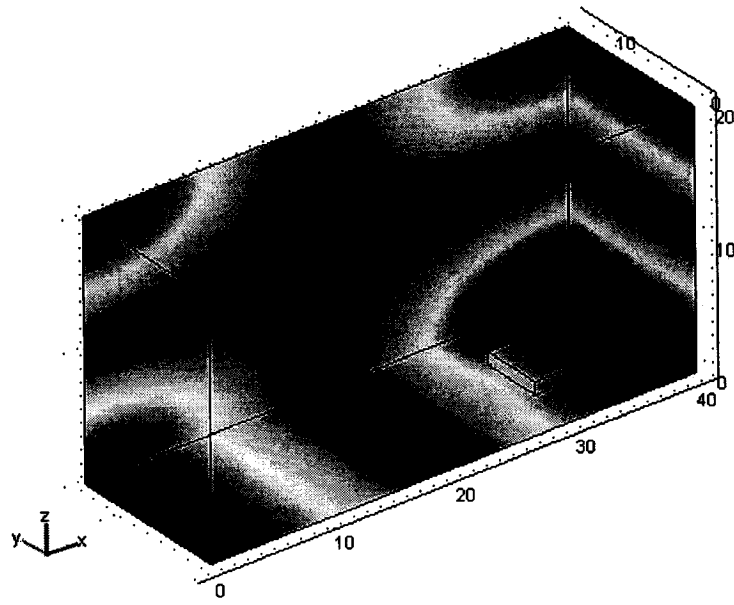


Figure 4-9 The pressure distribution for the eigenvalue,  $3.4e3$  (9.3Hz)

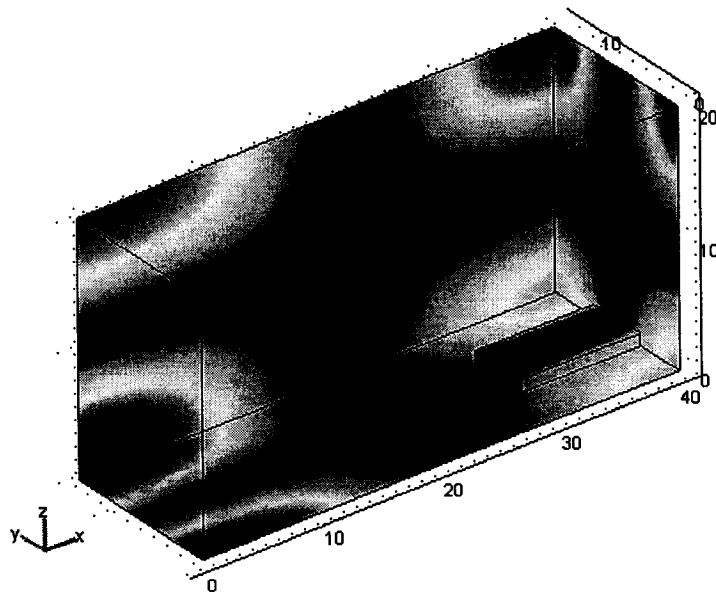


Figure 4-10 The pressure distribution for the eigenvalue,  $9.9e3$  (15.8Hz)

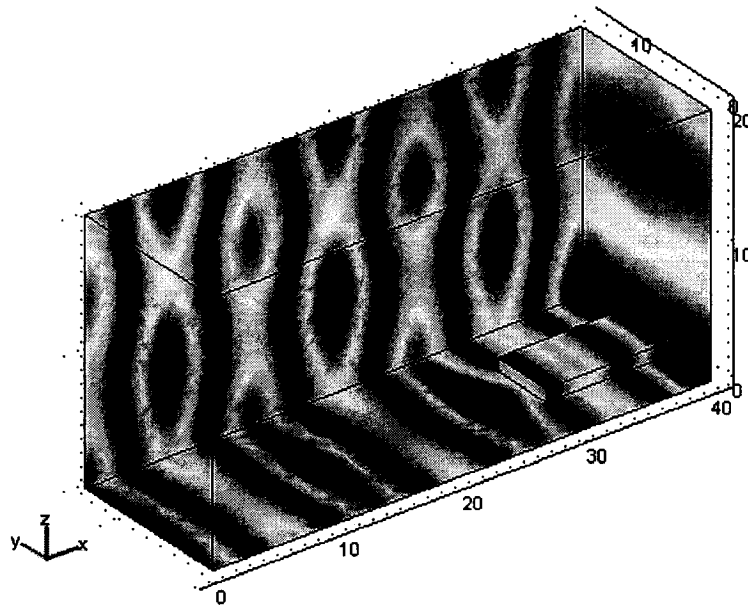


Figure 4-11 The pressure distribution for the eigenvalue,  $2.58e4$  (12.8Hz)

There is a special case for the mode  $(0, 2, 0)$ , which is showed in Figure 4-11. The reason is that the length of the room, which is 40.23 meters, is three times longer than its width, which is 13.41 meters, Then the eigenfrequency of mode  $(0,2,0)$  is the same as the eigenfrequency of mode  $(6,0,0)$ . The pressure distribution of these two modes has same patterns.

In order to describe the pressure distribution of the simulated room completely, the isosurface plot with the boundary plot for the pressure distribution in the room is necessary. Figure 4-12 shows the results with the isosurface and the boundary plot.

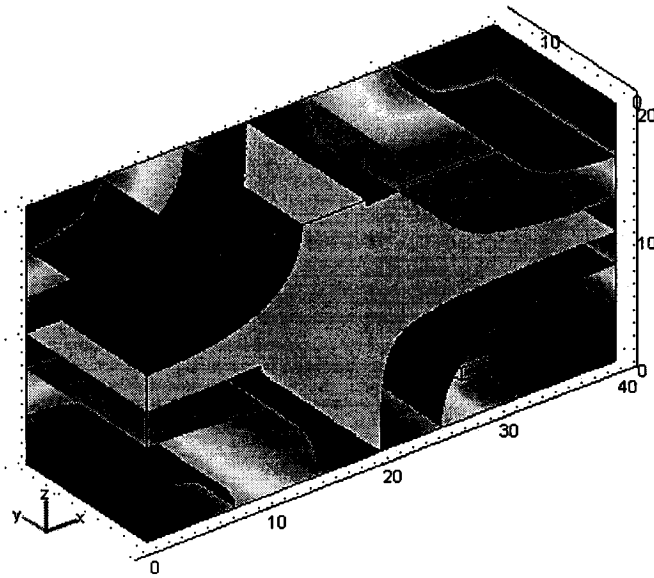


Figure 4-12 The pressure distribution for the eigenvalue,  $3.4e3$

Fig. 4-13 shows the results for the eigenfrequency, which is 80Hz. As mentioned before, if the sound frequencies are high, the sound field can't be described by the normal modes. Their use is significantly limited, due to the fact that they can be computed only for the lowest part of the audible frequency spectrum. Simulation study presented in next chapter is based, for this reason, on ray-based methods.

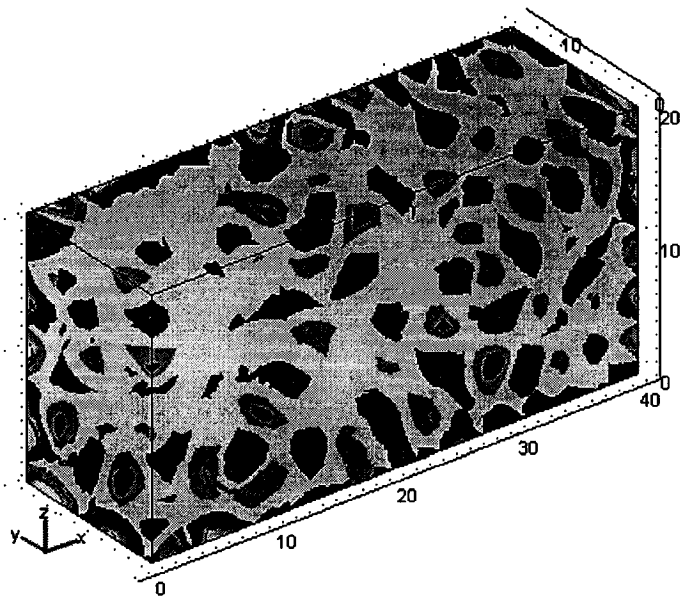


Figure 4-13 The pressure distribution for the eigenvalue,  $2.5e5$

## **Chapter 5**

### **Simulation Study of Room Acoustics**

Computer modeling is commonly used to predict acoustic performance. An early part of a response in a simulated room, based on the image method, is modeled in this chapter. The algorithms for the rectangular room, resulting response and analysis of modeling results are also presented.

#### **5.1 Image method**

The image method is one of the main methods in the geometrical acoustics. It applies the geometrical optics based on replacing the wave by a ray. However the sound and the light are total different phenomena. The sound is the propagation of the disturbances in the medium and can't travel without the medium, whereas the light is an electromagnetic wave that can propagate in vacuum, i.e., the material medium is not necessary for the propagation of the light. Another fundamental distinction between the light and the sound is their different velocities. The light travels at a speed of 299,792,458 meters per second. The velocity of the sound is about 300 meters per second. But they still have some similarities. For example, the light and the sound can be emitted in all directions. The most important similarity between the light and the sound is that both are forms of wave motion. As a

result, there are some important theories in optics, which can be applied for the sound propagation in acoustics, such as the law of the reflection from Huygens' Principle

In geometrical optics, the beam is defined a shaft of the light whose sides are parallel when it passes through a certain hole. If the size of the hole is sufficiently reduced, the beam of the light could be assumed a light ray, which travels in a straight line in the air [33]. The geometrical optics has three basic laws. The first is the law of the geometrical propagation, which states that the light ray moves in straight line. The others are the law of reflection and the law of refraction. The reflected ray follows the law of the reflection, which is showed in Fig. 5-1. The law can be stated as: the incident ray and the reflected ray lie in the plane containing the normal line and the angle of the reflected ray is equal to the angle of the incident ray.

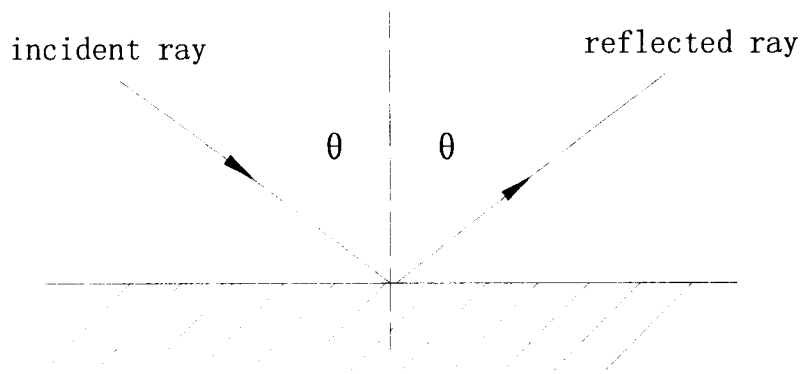


Figure 5-1 Reflection of the light ray

In 1670 the physicist Christian Huygens proposed a principle for the propagation of the light wave, which is known as Huygens' Principle [34]. This principle states that: all

points on a propagating wavefront are regarded as the sources of spherical secondary wavelets, which propagate in the forward direction at some later times. The envelope of the secondary wavelets constitutes the new wavefront. If the propagating wave has a frequency,  $f$ , and is passed through the medium at a speed,  $c$ , then the secondary wavelets will have the same frequency and speed.

In order to explain this principle clearer, a narrow parallel beam of the light (ABC) is considered. Fig. 5-2 [35] shows that a wavefront ABC encounters a smooth hard wall ( $X-Y$  plane) at an angle  $\Phi$  with the normal to that wall. All points along the wavefront don't reach the wall at the same time. The first point reaches the wall at the point  $A'$ . The point  $A'$  serves as a source centre and a secondary wave is produced, that reaches  $A''$  when the ray from  $C$  reaches the wall at  $C'$  and this defines a circle of radius  $C'C''$ . When the ray from  $B$  reaches at a point  $B'$ , another secondary wave is produced. The radius is reduced, because the ray  $BD$  travels from  $D$  to  $B'$  before reflection. Actually there are many wavelets during the same time interval. The radii are reduced gradually until the time becomes zero, when the wavefront reach the wall at the point  $C'$ . Then the reflected wavefront  $A''B''C'$  is the envelope of these wavelets. It is easy to prove that  $A'A'' = C'E$ . The incident light ray  $CC'$  is perpendicular to the wavefront  $A'DE$  and the reflected ray  $A'A''$  is also perpendicular to the reflected wavefront  $A''B''C'$ . The angle  $\Phi$  is the normals to the incident light and the reflected light with respect to the wall. Hence,

$$\text{Angle of the reflected light} = \text{Angle of the incident light}$$

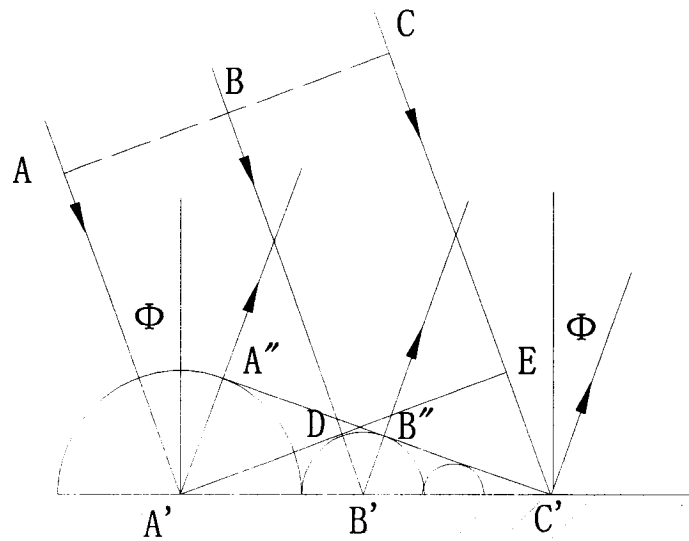


Figure 5-2 The reflection of a beam of the light on a smooth hard wall

In acoustics, the reflection of the sound waves obeys the laws developed by optics discussed above. However, the speed of the light is very high and the wavelengths of the light wave are very small compared with the dimensions of the reflected surface. Therefore, most of the geometrical principles of the light ray can be applicable to the sound waves of high frequencies. In other words, if the wavelength of the sound wave is very small compared with the dimension of the reflected surfaces, the geometrical optics can be applied for this kind of the sound wave. Fig. 5-3 [35] illustrates a spherical sound wavefront radiating from a point source on the smooth hard wall. If the dimension of the source is very small compared with the wavelengths radiates, it is called a point source, which radiates in all directions and forms increasing circles from the center of the source. According to Huygens' Principle, the reflected wavefront  $W$  is the enveloping line. It is convenient to see that the wavefront  $W$  can be obtained by an additional source of source  $S_1$ , which is a mirror

image to the source  $S_o$  behind the wall. The wavefront  $W$  may be represented as if it radiates directly from the image source  $S_i$  in free space.

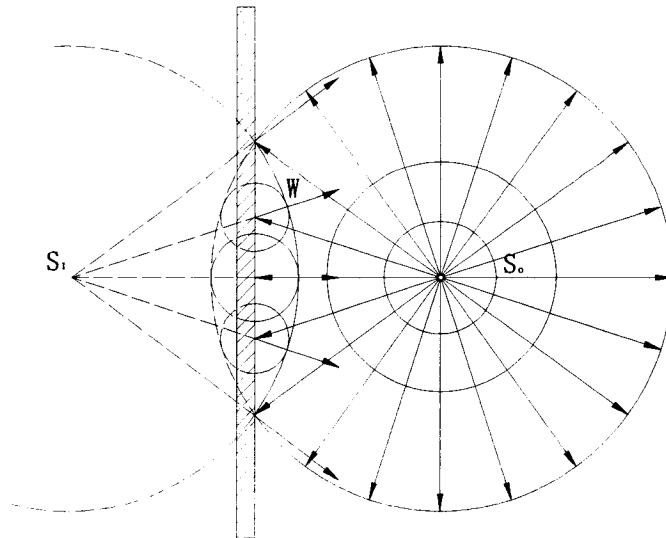


Figure 5-3 Spherical waves from a point source and are reflected by a hard wall

By employing the concept of the mirror-like reflection, the sound field may be described at a simplified way in the geometrical acoustics, especially for the enclosed spaces. This is also called the image method in geometrical acoustics. The image method is efficiently applied for a source-to-receiver impulse response.

## 5.2 Simulation model

In geometric acoustics, a sound ray replaces the sound wave. This assumption is acceptable for the very short wavelengths relative to the dimensions of the room and its objects. For example, for a frequency of 1000Hz with a wavelength of 34cm, this approximation geometric acoustics can be used for modeling room.

The simulation model is assumed for a rectangular room assumed as a homogeneous medium. The surfaces of the room are considered smooth and hard. The refraction phenomena don't occur in the room and diffraction is also neglected. Further, the propagation of the sound ray is in the straight line until it encounters the surfaces of the room. Fig. 5-4 shows that a sound source S that has a certain distance from a surface reflects from the surface and reaches the receiver R. The receiver R receives two signals, one is the direct path and the other is the reflection path. The length of the direct path (SR) can be directly calculated from the distance between the sound source and the receiver. For the reflection path, we assume an image source S', which is located opposite at the surface, that radiates the same sound signals as the sound source S and their directional characteristics are also same. The distance of the image source S' from the surface is equal to the distance of the real source S from the surface. Then, S' is connected to R and P is the point of intersection of S'R with the surface. Because the image source S' is symmetrical to the real source S, the length of the reflection path SP+PR is the same as S'R. As a result, we can compute the distance between the receiver and the image source for calculation the length of the reflection path. This is the case that involves one reflection in the path.

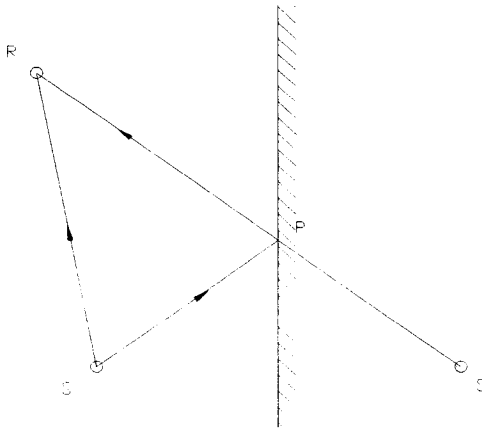


Figure 5-4 A source with one level images

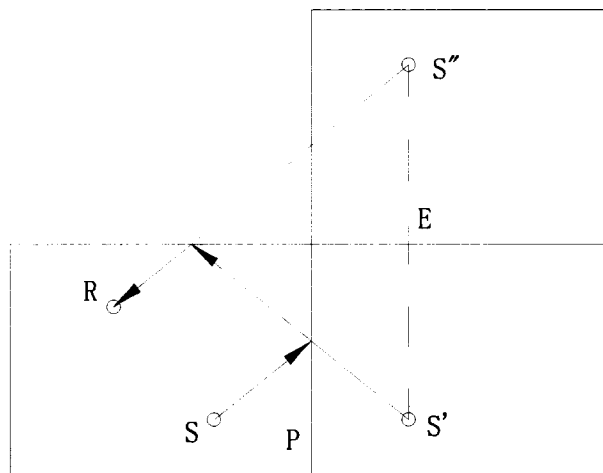


Figure 5-5 Reflection paths with two levels of images

Now we consider a sound ray that originated from a sound source in a rectangular room. If the room is bounded by plane surfaces, it is convenient to construct the image source to calculate the length of the ray path. A rectangular room has six surfaces and each

surface is associated with one image of the original sound source and each wall mirrors each of these image sources of first order. By repeating this procedure again and again, there will be an infinite number of sources. Fig. 5-5 shows the reflected sound involving two reflections. The length of the reflection path can be calculated directly from the distance  $RS_2$ . In Fig. 5-6 the reflection path involving three levels of images can be obtained from the length  $S_3R$ . Fig. 5-7 shows that the four assumed rooms adjacent to the sides of the original room have one first-order image source each. There are four assumed rooms adjacent at the corners of the original room that have a second-order image source.

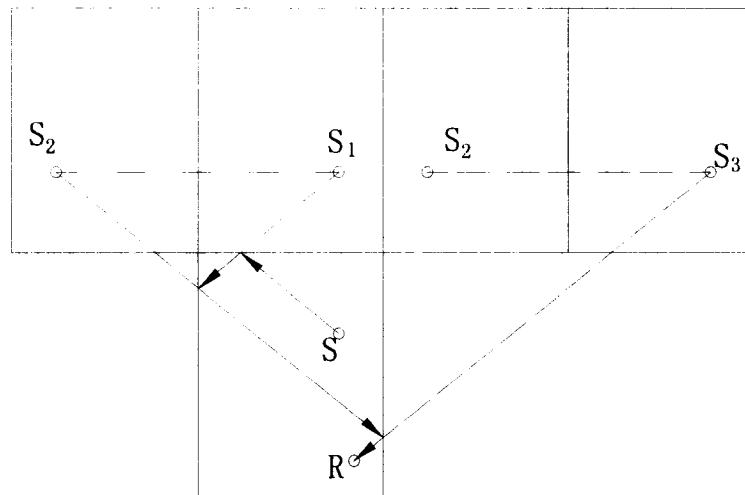


Figure 5-6 Reflection path involving three levels of images

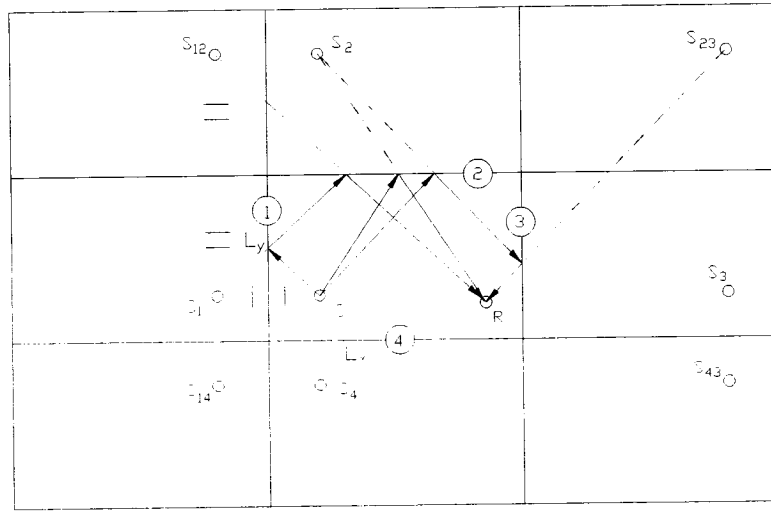


Figure 5-7 A sound source with different levels of images

The image model can be used to do the simulation in a digital computer. Jont B. Allen and David A. Berkley have developed an efficient method to make an impulse response for a rectangular room by constructing image sources

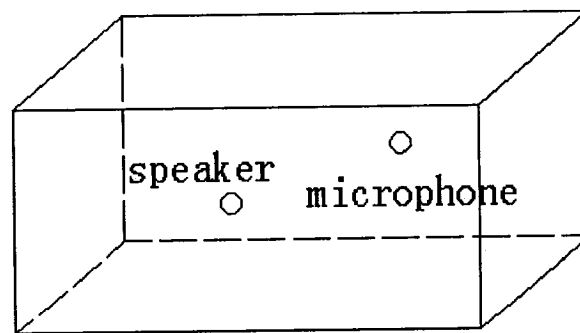


Figure 5-8 The simulation model

The rectangular room showed in Fig. 5-8 corresponds to the size of the Solomon Temple and Sixtine Chapel and used as the simulated room. The dimensions of the room are  $L_x = 40.23m$ ,  $L_y = 13.41m$ ,  $L_z = 20.70m$ . A speaker is assumed as an omnidirectional point source, which radiates the signals with equal intensity in all directions, and a microphone is modeled as a receiver. Consider this room in the  $x$ ,  $y$ , and  $z$  directions of a rectangular coordinate system, the origin of which is at the room centre. The speaker is located at  $(x_s, y_s, z_s)$  and the microphone is located at  $(x_r, y_r, z_r)$ . We assume that each surface of the room is a plane and, that the walls are smooth surfaces, which are rigid. We use image methods to simulate the impulse response between the source and the receiver in this room. As we know, the microphone will receive signals not only by the direct path but also by numerous different reflection paths from various directions. This means that there will be an infinite number image sources that we have to construct. The image method only includes contributing images that are in a sphere with radius given by the speed of sound times the interval time ( $R = c \times t$ ). The image sources located outside  $R$  do not influence the sound field in the room for time interval  $[0, t]$ . Fig. 5-9 is a 2-dimensional slice that includes the original room, with the sound source, and indicates how image sources are spatially arranged [4]. Actually, the image pattern should be expressed in a 3-dimensional space, i, e, a third dimension must be considered. Along the third dimension there are some similar patterns at equal distances  $L_z$  in this sphere. The impulse response of this room can be simulated by the assumption that all images in this sphere generate the signals, which are the same as the original source, when the time  $t = 0$ . Since each of the images travels on a different path, the reflections reach the receiver at different times that represent as the delayed times with respect to the direct sound. Also, they have different strengths, which are dependent

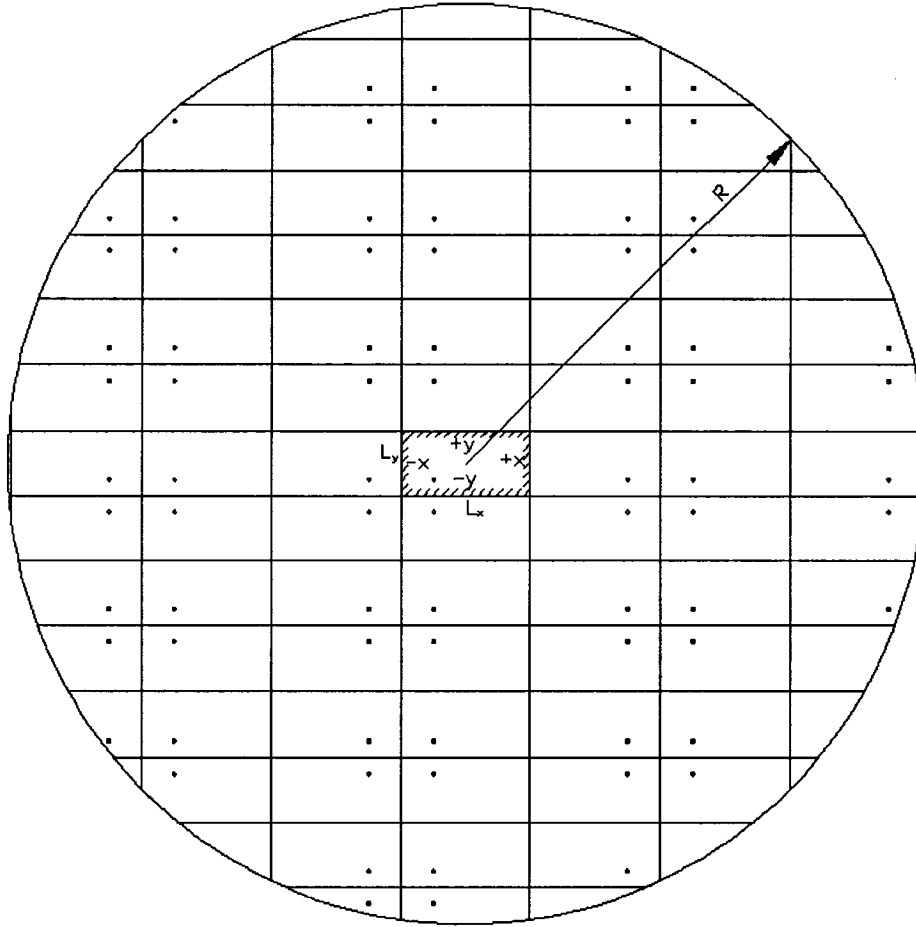


Figure 5-9 Image sources in a rectangular room

to the lengths they cover. In order to compute the length of the paths, the location of the images must be found. The locations of the image source will be [22]

$$x_{nlm} = nL_x + (-1)^n x_s$$

$$y_{nlm} = lL_y + (-1)^l y_s$$

$$z_{nlm} = mL_z + (-1)^m z_s$$

where  $n, l, m = 0, \pm 1, \pm 2, \dots$

This can be expressed by considering the reflection of the source by the  $-x$  and  $+x$  walls. For example, the first order of image generated by the  $+x$  wall is given by

$$\frac{L_x}{2} + \left(\frac{L_x}{2} - x_s\right) = L_x - x_s$$

This corresponds to  $nL_x + (-1)^n x_s$  with  $n=1$ .

The first order of image generated by  $-x$  wall is given by

$$-\frac{L_x}{2} + \left(-\frac{L_x}{2} - x_s\right) = -L_x - x_s$$

This corresponds to  $nL_x + (-1)^n x_s$  with  $n=-1$

The second order of image generated by  $+x$  wall is the reflection of the image ( $n=-1$ ),

$$\frac{L_x}{2} + \left[\frac{L_x}{2} - (-L_x - x_s)\right] = 2L_x - x_s$$

This corresponds to  $nL_x + (-1)^n x_s$  with  $n=2$ .

The second order of image generated by  $-x$  wall is the reflection of the image ( $n=2$ ),

$$-\frac{L_x}{2} + \left[-\frac{L_x}{2} - (2L_x - x_s)\right] = -2L_x - x_s$$

This corresponds to  $nL_x + (-1)^n x_s$  with  $n=-2$ .

The procedure is repeated until the high-order image sources we need to construct.

The  $n$  order of image, with  $n$  positive, generated by  $+x$  wall is the reflection of the image ( $n-1$ ).

$$\frac{L_x}{2} + \left\{\frac{L_x}{2} - [(-n+1)L_x + (-1)^{-n+1} x_s]\right\} = nL_x + (-1)^n x_s$$

The  $n$  order image, with  $n$  negative, generated by  $-x$  wall, is the reflection of the image ( $-n-1$ ).

$$-\frac{L_x}{2} + \left\{ -\frac{L_x}{2} - [(-n-1)L_x + (-1)^{n-1}x_s] \right\} = nL_x + (-1)^n x_s$$

Similar considerations can be applied to the  $y$  and  $z$  components.

We assume that the sound source radiates a unit pulse. According to Eq.5-1, the impulse response function for this speaker and microphone in the simulated room can be rewritten as [13] [36] [37]

$$h(t, X, X') = \sum \frac{\delta(t - D/c)}{4\pi D} \quad (5-1)$$

where

$D$  expresses the distance between each image source to the receiver.

$c$  is the sound speed in the air.

$$X = x_s, y_s, z_s$$

$$X' = x_r, y_r, z_r$$

$D/c$  means a time delay that each image source renders the signal to the receiver.

$1/4\pi D$  indicates the strength attenuation compared with the strength of original sound.

$\sum$  represents that summation that provides the impulse response should include every image source in the sphere whose radius is  $c \times t$ .

These results are based on the assumption that the surfaces of the room are rigid. If the surfaces of the room aren't rigid and have reflection coefficients, each surface absorbs certain part of the signal when it encounters the surface. Assuming that  $\beta_{-x}, \beta_{+x}, \beta_{-y}, \beta_{+y}, \beta_{-z}, \beta_{+z}$  are the reflection coefficients of the room, the room impulse response function can be given by [22]

$$h(t, X, X') = \sum \frac{A_{nlm} \delta(t - D/c)}{4\pi D} \quad (5-2)$$

where

$$A_{nlm} = a_n a_l a_m$$

$$a_n = \beta_{-x}^{\frac{|n|}{2}} \beta_{+x}^{\frac{|n|}{2}} \quad \text{for } n=\text{even}$$

$$a_n = \beta_{-x}^{\frac{|n-1|}{2}} \beta_{+x}^{\frac{|n+1|}{2}} \quad \text{for } n=\text{odd}$$

$$a_l = \beta_{-y}^{\frac{|l|}{2}} \beta_{+y}^{\frac{|l|}{2}} \quad \text{for } l=\text{even}$$

$$a_l = \beta_{-y}^{\frac{|l-1|}{2}} \beta_{+y}^{\frac{|l+1|}{2}} \quad \text{for } l=\text{odd}$$

$$a_m = \beta_{-z}^{\frac{|m|}{2}} \beta_{+z}^{\frac{|m|}{2}} \quad \text{for } m=\text{even}$$

$$a_m = \beta_{-z}^{\frac{|m-1|}{2}} \beta_{+z}^{\frac{|m+1|}{2}} \quad \text{for } m=\text{odd}$$

This can be described as if the nth image is generated by alternative reflections by the  $-x$  and  $+x$  surfaces. The strength of each reflection is multiplied by the reflection coefficient of the reflecting surface. Then, when  $n$  is even, half of the reflection will be from the  $-x$  surface and another half of the reflection will be from the  $+x$  surface. The factor is modified by

$$a_n = \beta_{-x}^{\frac{|n|}{2}} \beta_{+x}^{\frac{|n|}{2}}$$

when  $n$  is odd. If  $n$  is positive, the last reflection should be  $+x$  wall. Otherwise, while  $n$  is negative, the last reflection would be  $-x$  wall. Then the factor is given by

$$a_n = \beta_{-x}^{\frac{|n-1|}{2}} \beta_{+x}^{\frac{|n+1|}{2}}$$

Similar considerations are applied to the  $y$  and  $z$  component.

### 5.3 Simulation results

The impulse response for this room was computed with Matlab software. Fig. 5—10 shows the flow chart of Matlab program. We assume that the omnidirectional source emits at time  $t = 0$  an infinitesimal short pulse whose amplitude is 1. The location of source is at -1, -1, -1 and the location of the receiver at 5, 2, -5. A schematical reflection diagram is plotted. In the diagram, the abscissa is the delay time of a reflection and the ordinate is the strength of the reflection. For the case that the surfaces of the room are rigid the results are displayed in Fig. 5-11. When  $t = 0$ , the real source and the image sources simultaneously radiate the pulse. The first sound that reaches to the receiver is the direct sound and the strength of the direct sound is larger than any of the reflected sound due to the shortest distance between the source and the receiver. Because the surfaces are rigid, the surfaces don't absorb when the sound ray strikes them and reflects from them. The amplitude is reduced as  $1/r$  in every spherical wave. As shown in Fig. 5-11, the early part of the reflections has distinct reflection arrivals, because of the relatively small number of image sources generated in the short time duration. As the time goes on, the density of the reflection arrivals increases rapidly and individual reflections will no longer be separated from each other. For the case that the surfaces of the room aren't rigid, for example when the reflection coefficients of ceiling and floor are 0.7, and the others are 0.9, the results are showed in Fig. 5-12.

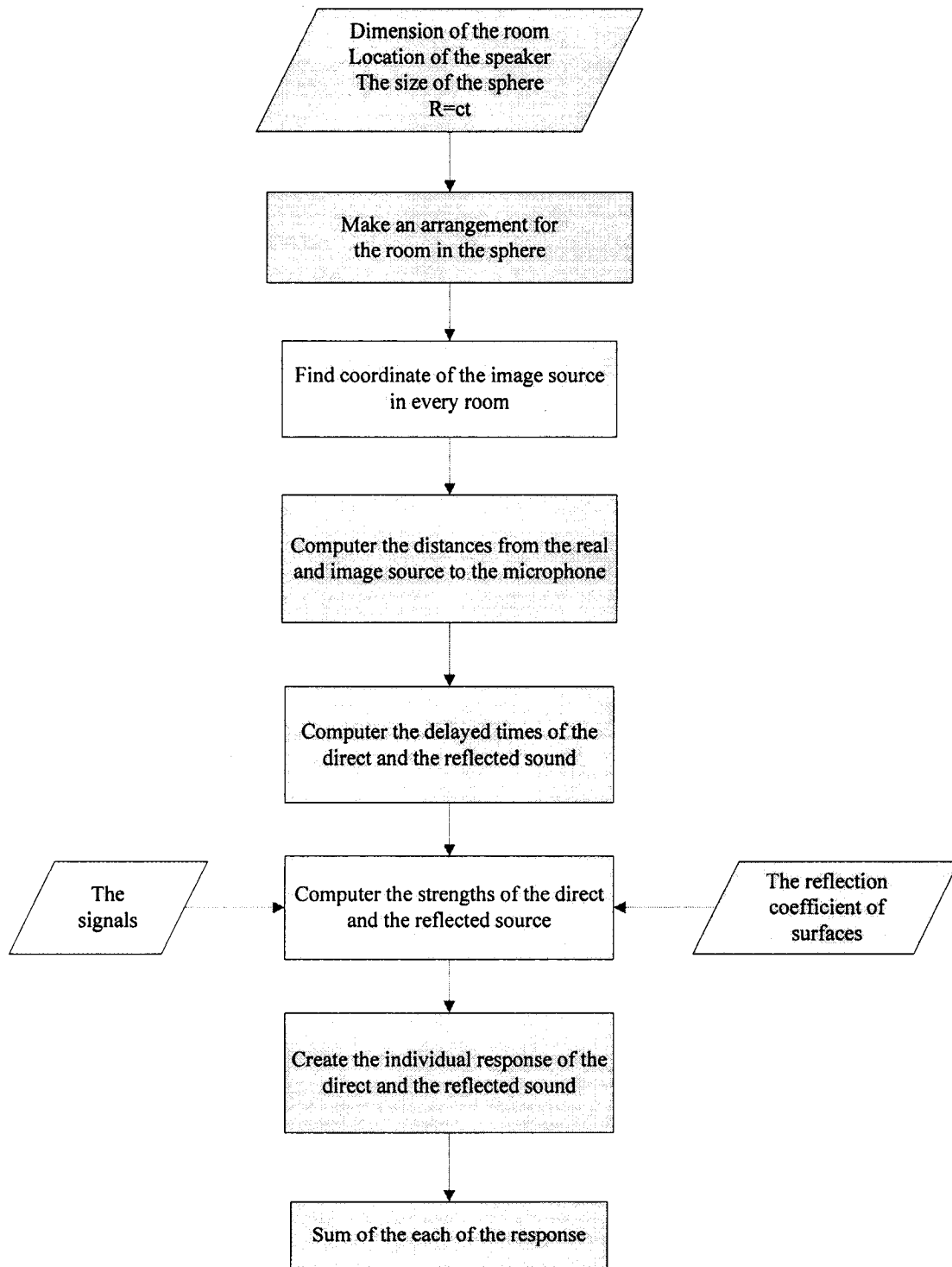


Figure 5— 10 The flow chart of Matlab program

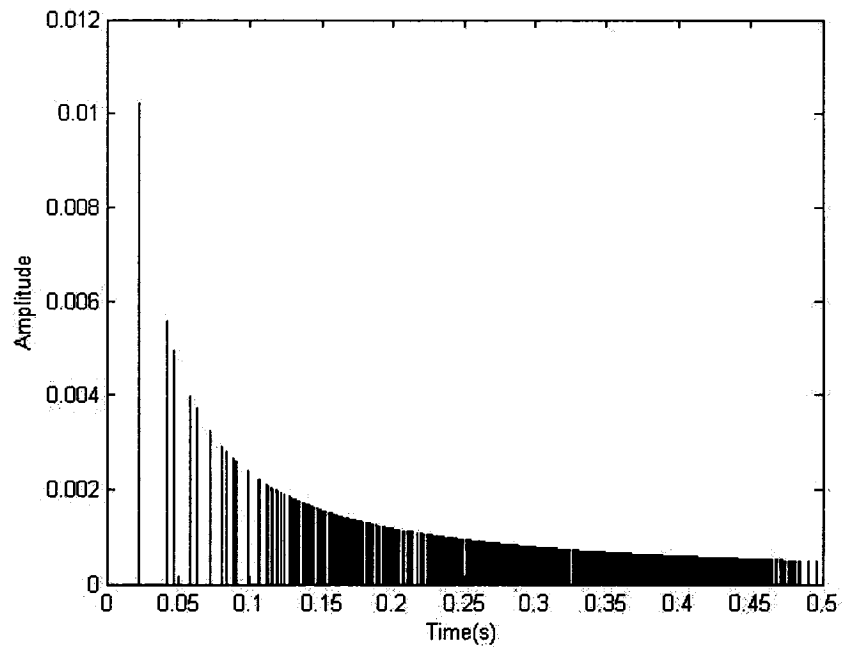


Figure 5-11 Reflection diagrams for the room with rigid surfaces

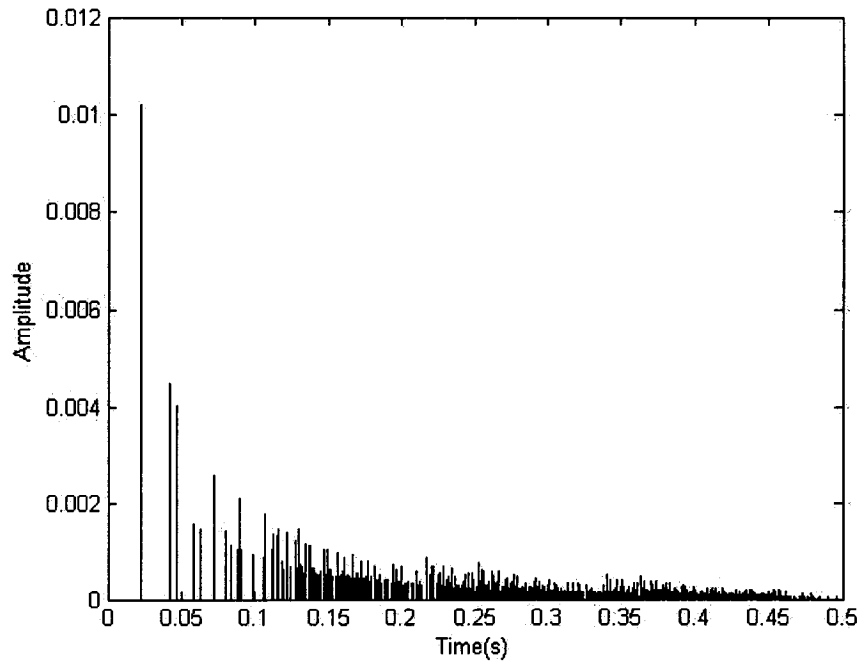


Figure 5-12 Schematical diagram for the room with nonrigid surfaces

The difference between Fig. 5-11 and Fig. 5-12 is the attenuation of the signal in the room with nonrigid surfaces. The reason is that certain part of the signal is absorbed by the surfaces when the signal is reflected from nonrigid surfaces. The reflection diagram contains all significant information on the temporal structure of the sound field at a certain room point.

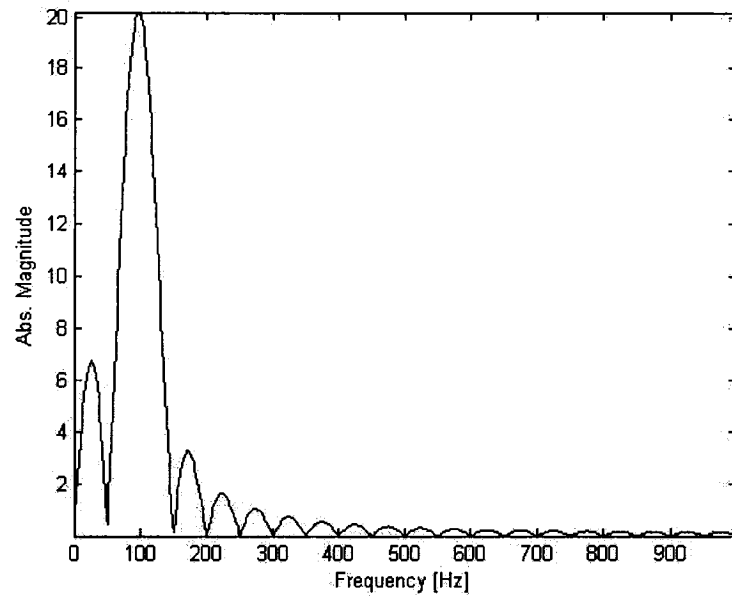


Figure 5-13 Frequency spectrum for one cycle of the sine wave  $x = \sin 200\pi t$

Considering that source is more complicated than a unit pulse, a cycle of a sine wave  $x = \sin 200\pi t$  is next applied, shown in Fig. 5-13. This kind of the sine wave can be expressed as the pulse sine wave due to the short duration, which includes a sine wave and a square wave. Consequently, the spectrum is a combination of the spectrum for a sine wave (100Hz) and the spectrum for a square wave, which is a series of harmonics. When source is turned on, we calculated the impulse response at the receiver between 0 and 400ms. The results are displayed in Fig. 5-14 and Fig. 5-15. In Fig. 5-14 we assume that the six surfaces of the room are rigid. In Fig. 4-15 we suppose that the wall reflection coefficients are all 0.9

and ceiling and floor coefficients are 0.7. The first sine wave seen clearly is the direct wave. The amplitude of the direct sine is same in both diagrams before the first reflections.

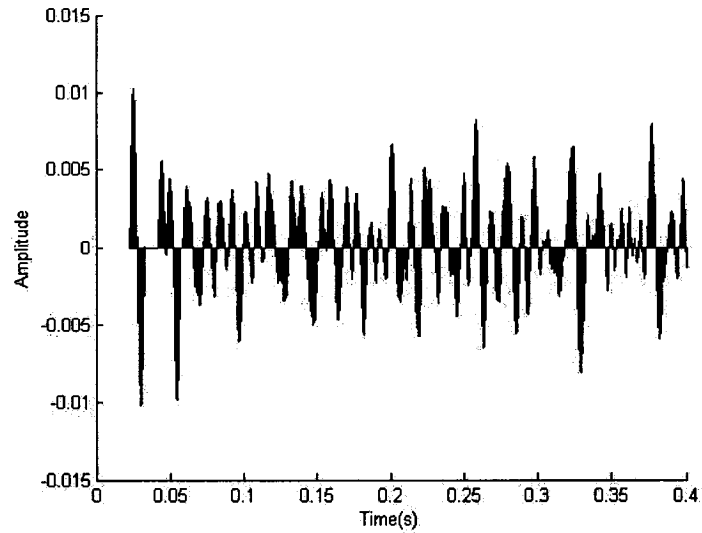


Figure 5-14 Receiver signal for one cycle of the sine wave

$$x = \sin 200\pi t \text{ for a room with rigid walls}$$

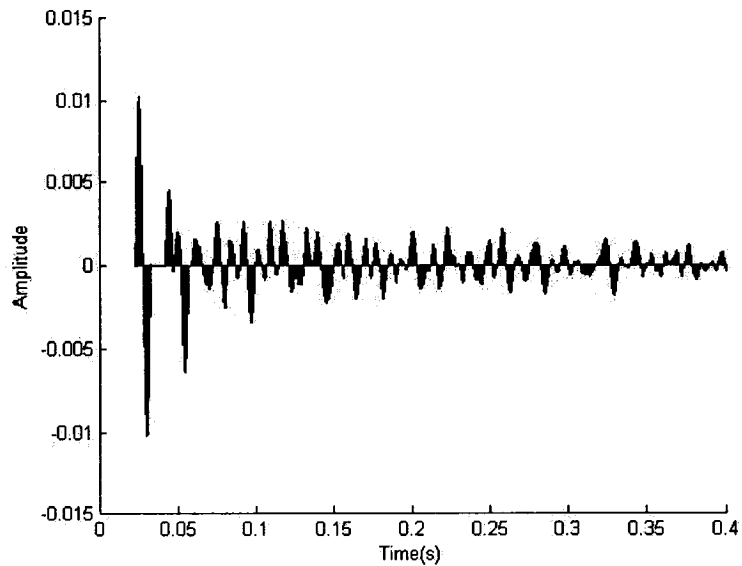


Figure 5-15 The reflection diagram for one cycle of the sine wave,  $x = \sin 200\pi t$  in the case of nonrigid walls

Next we consider the source,  $x = \sin 2000\pi t$ , shown in Fig. 5-16. The results are shown in Fig. 5-17 and Fig. 5-18. In Fig. 5-17 we plot the impulse response for this room with rigid surfaces. In Fig. 5-18 we consider that the wall reflection coefficients are all 0.9, and that the ceiling and floor coefficients are 0.7. As seen in Fig. 5-17 and in Fig. 5-18, the direct wave and the several early reflected waves have distinct arrival times because there few reflections happened during the early time and the length of this sine wave is smaller than the interval time required for the reflected waves to reach the receiver. However, numerous reflections arrive at a later time.

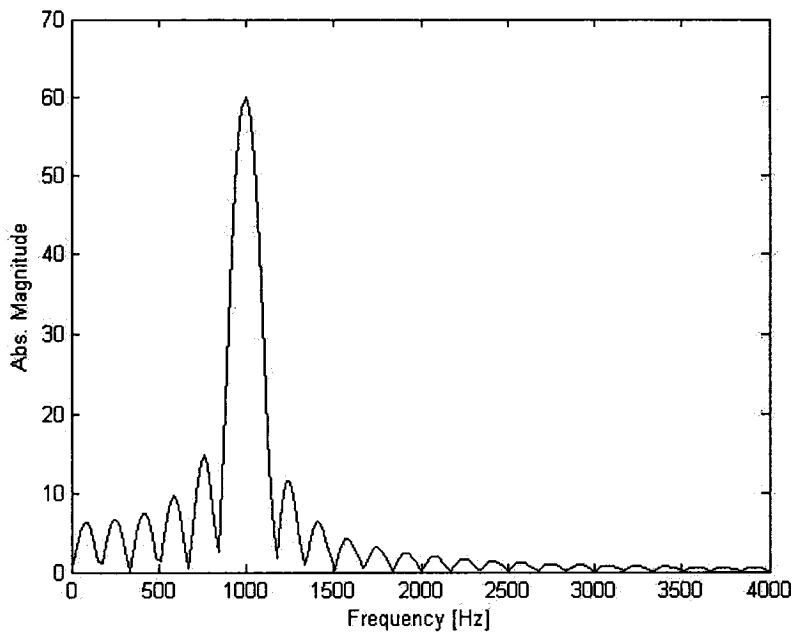


Figure 5-16 Frequency spectrum for one cycle of the sine wave  $x = \sin 2000\pi t$

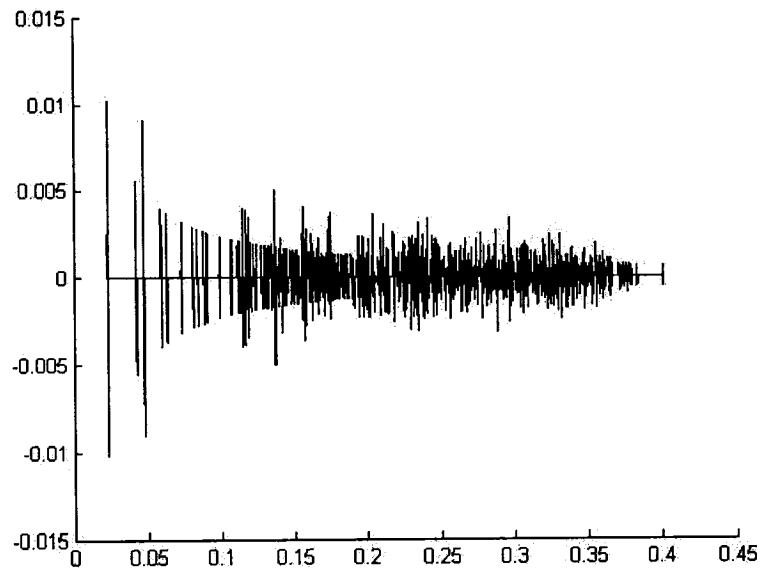


Figure 5-17 The reflection diagram for the sine wave  
 $x = \sin 2000\pi t$  for nonrigid walls

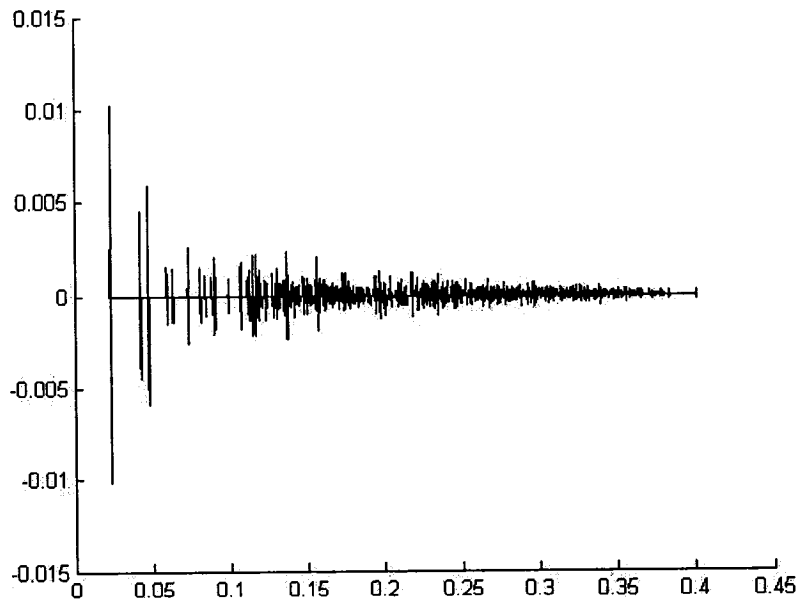


Figure 5-18 The reflection diagram for the sine wave  
 $x = \sin 2000\pi t$  for nonrigid walls

Further simulation studies were carried out for the source sound signal shown in Fig. 5-19. The signal was selected from [45]. This signal has the frequency spectrum shown in Fig.5-20. The lowest part of human voice frequency is higher than 100Hz. According to the dimension of the simulated room the signal is satisfied the assumption of the image method. The locations of the source and the receiver are same as before. Matlab program sound.m from appendix can read the sound file and we can get sound data and sample frequency. Then these data input give the impulse response of the room ( Result\_sound.m for details). Fig.5-21 shows the signals the microphone receives in this room with rigid surfaces. The results for the room with nonrigid surfaces are displayed in Fig.5-22. The reflection coefficients of the four walls are all 0.9; while ceiling and floor coefficients are 0.7. We save two different outputs into the sound files, which are echo.wave for rigid surfaces and reverberation.wave for nonrigid.wave.

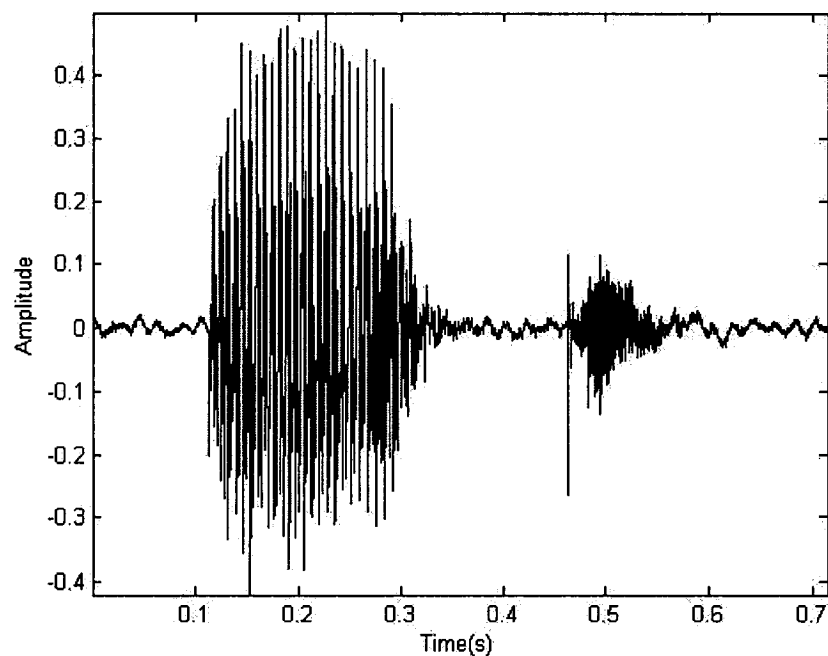


Figure 5-19 The sound signals for the input

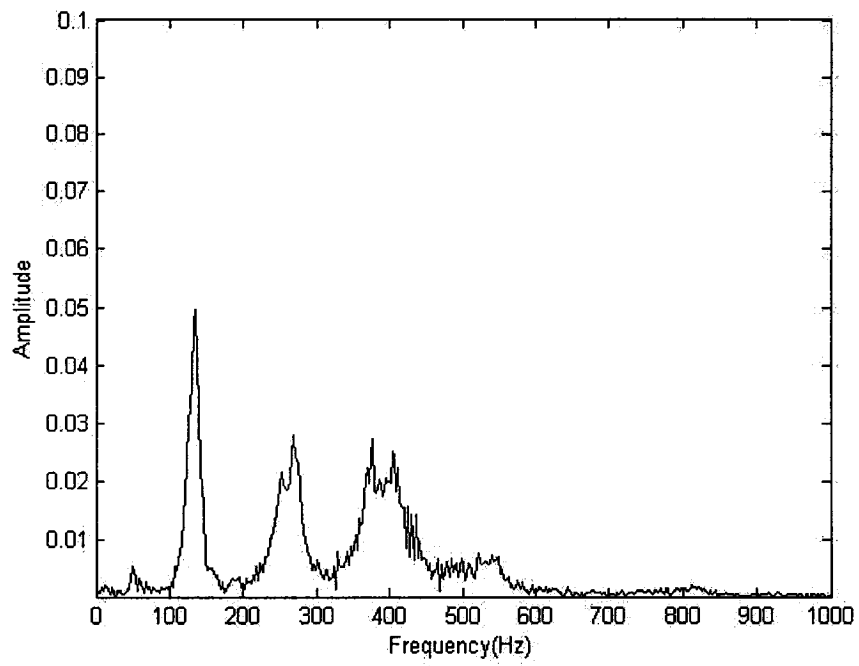


Figure 5-20 The frequencies of the input signals

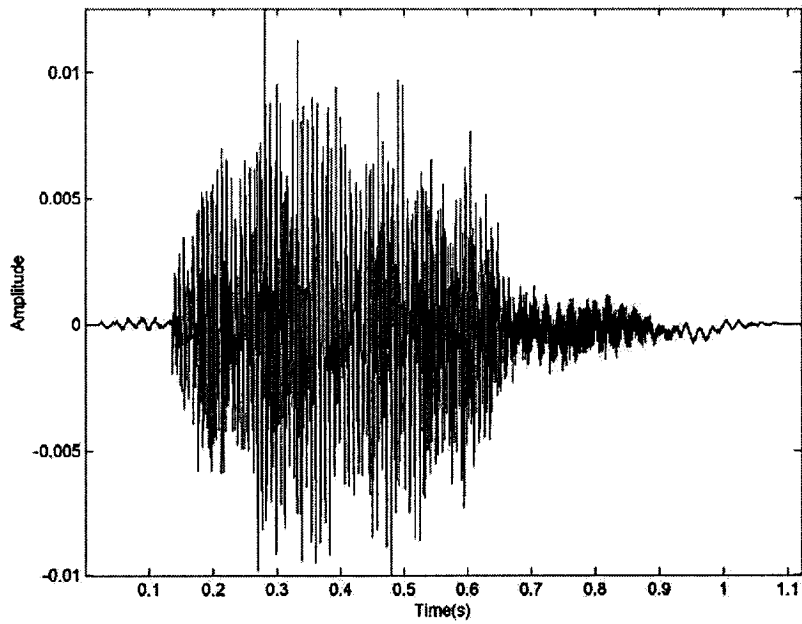


Figure 5-21 Response for the room with rigid walls

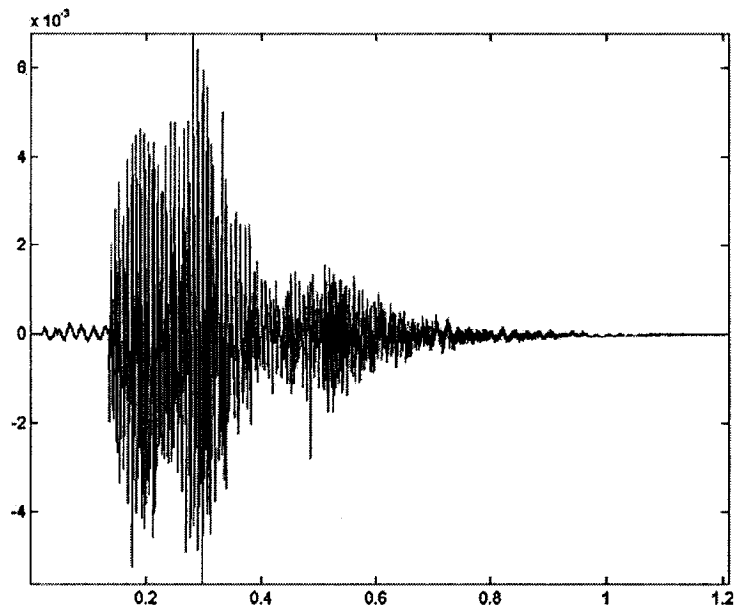


Figure 5-22 Response for the room with nonrigid walls

Compared with these two charts, the contribution of the reflected sound to the total strengths of the sound receiving the microphone can exceed the contribution of the direct sound if the surfaces of the room are fully reflective. This can lead to echo phenomena in a long time and to a poor sound quality.

We consider further that the source is in anechoic room. The location of the source and the receiver are same in Cartesian coordinates, and there is no reflection in this case. The signal consists only of the direct wave from the sound source. The signal the receiver receives has a time delay and the amplitude of the signal is in inverse proportion to the distance between the sound source and the receiver. The result is shown in Fig.5-23 and saved in the sound file: sound in anechoic room.wav. Compared with the input signals in Figure 5-19, it can be seen that the figures of two signals are same. However the amplitudes

in anechoic room are less than that of the original signals. Without reflection the sound is weak.

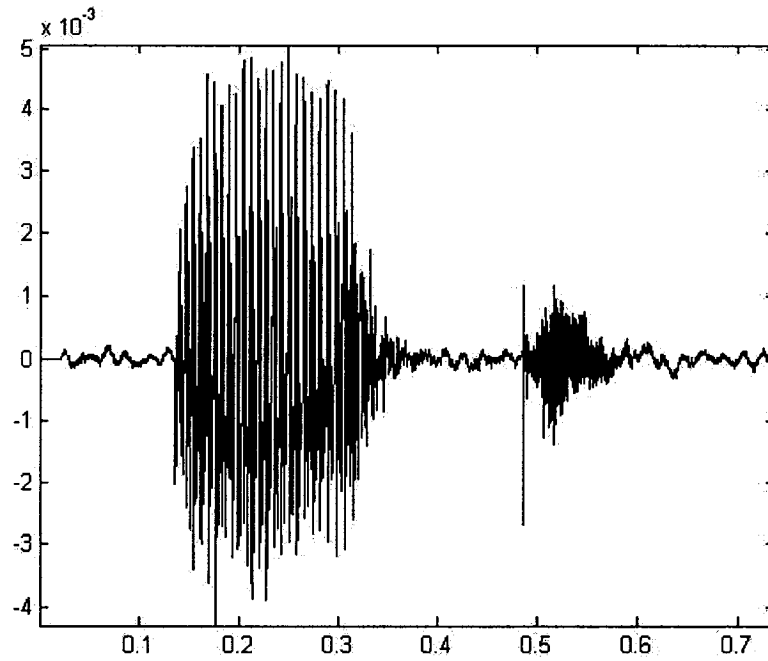


Figure 5-23 The impulse response in the anechoic room

The conclusion is that the simulation results prove to be plausible and, consequently, simulation is used further in this research for designing the experiments.

## **Chapter 6**

### **Experimental study of the room acoustics**

An acoustic experiment for the measurement of the response in an enclosure is presented in this chapter. Digital signal processing for this experiment set up and the programs for displaying the results, as well as the basic digital processing techniques and theories, such as Fourier transform and the lower-pass digital filter, are summarized in this chapter..

#### **6.1 Sound card**

A sound card is used to generate the high quality sound. A computer with a sound card can capture and record the sound from external sources. Even though there are many types of sound cards, most of sound cards have four fundamental components.

- An analog-to-digital converter
- A digital-to-analog converter
- An interface that connect the sound card to the motherboard of the computer
- Input and output that connect to a microphone and speaker.

The software associated with the sound card is based on digital signal processing.

Digital signal processing is the processing of the signals in digital form. The digital processing of an analog signal contains basic three steps. First the analog signal must be

converted into a digital form and processed for the digital version. Then the processed digital signal is converted back into an analog form as an output, as illustrated in Fig.6-1 [38][39].

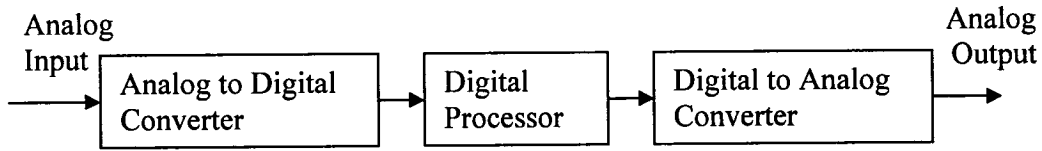


Figure 6-1 Scheme for the digital processing of an analog signal

The sound card deals with sound. The sound produced by the microphone or some other transducer is analog, i.e., different from the computer data. The sound wave must be converted into digital data that can be acquired by the computer before digital signal processing can be applied.

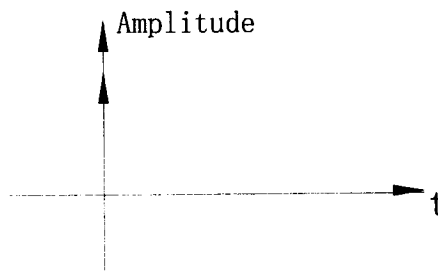


Figure 6-2 The pulse signal

The sampling can be described as a multiplication of an analog input signal with impulse function [40]. Fig. 6-2 shows a unit pulse signal. The impulse function for this signal is supposed that a rectangular pulse whose width is infinitesimally small and the amplitude is the result of the condition.

$$\int_{-\infty}^{\infty} \delta(t) dt = 1 \quad (5-1)$$

The sampling waveform would be the sum of all individual impulse function with evenly discrete time  $t_s$ , as illustrated in Fig.6-3.

$$x(t) = \delta(t - \infty) + \dots + \delta(t - t_s) + \delta(t) + \delta(t + t_s) + \dots + \delta(t + \infty) \quad (5-2)$$

Also

$$x(t) = \sum_{n=-\infty}^{\infty} \delta(t - nt_s) \quad (5-3)$$

where  $x(t)$  is the sampling function.

Considering an analog input signal  $f(t)$ , shown in Fig.6-4, the sampled signal  $y(t)$  (Fig.6-5) can be obtained by the multiplication of  $x(t)$  with the input analog signal  $f(t)$ :

$$y(t) = \sum_{n=-\infty}^{\infty} f(t) \cdot \delta(t - nt_s) \quad (5-4)$$

The most important thing for transforming a continuous-time signal into a discrete-time signal is the sampling time  $t_s$ . Shannon's sampling theorem states that an analog signal can be represented accurately if the minimum sampling frequency is equal to or greater than twice the highest frequency of the signals. The highest frequency is referred to as the Nyquist frequency. If the maximum frequency of the analog input is  $f$ , the sampling frequency  $f_s \geq 2f$  (where  $f_s = 1/t_s$ ). When  $f_s < 2f$ , an aliasing phenomenon will occur, which results in a poor representation of the analog signal.

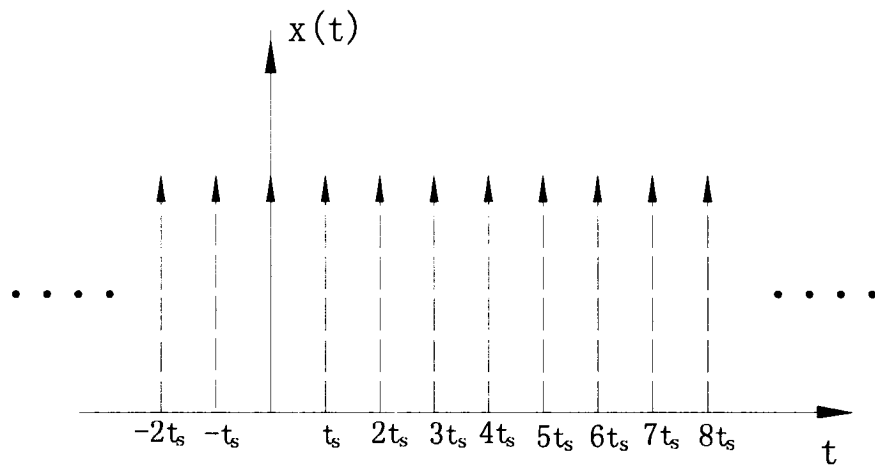


Figure 6-3 The individual impulse function with evenly time period

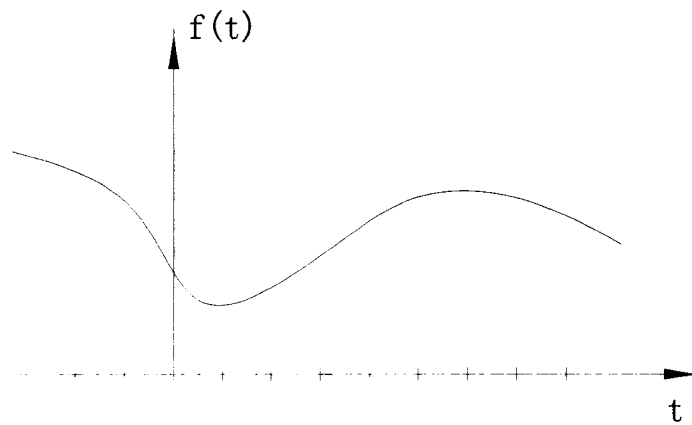


Figure 6-4 The analog input signal

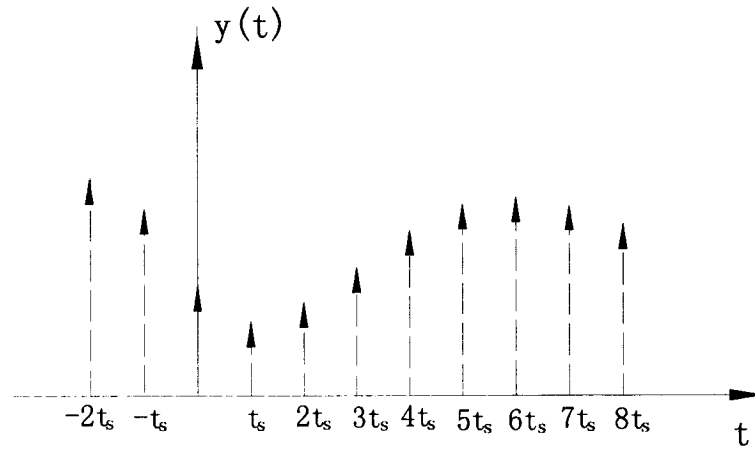


Figure 6-5 The sampled input signal

Quantizing must be performed using the sampling and hold steps. The sampled signals are quantized into bits, which can be read by the digital computer. The more digital levels an ADC (analog-to-digital converter) has, the more accurate signals we can get.

When we play the digital signals back through the speaker, the digital-to-analog converter would perform same basic steps in reversed order. In chapter 5 simulation results under different conditions were saved as wave files. These wave files can be converted into the analog signals by the sound card and we can verify the simulation results directly by the sound that is from the output of sound card.

## 6.2 The experimental setup

The room used for the experiment is a rectangular empty room with the dimension by 9.4 by 1.88 by 2.2 meters. The location of the sound source is at -1.2, 0.14, -0.5 and the location of the microphone is -3.1, -0.4, -0.21 in a Cartesian coordinate system with the

origin is at the room centre. The reflection coefficients of the walls are approximated as 0.98. The others are approximated as 0.99.

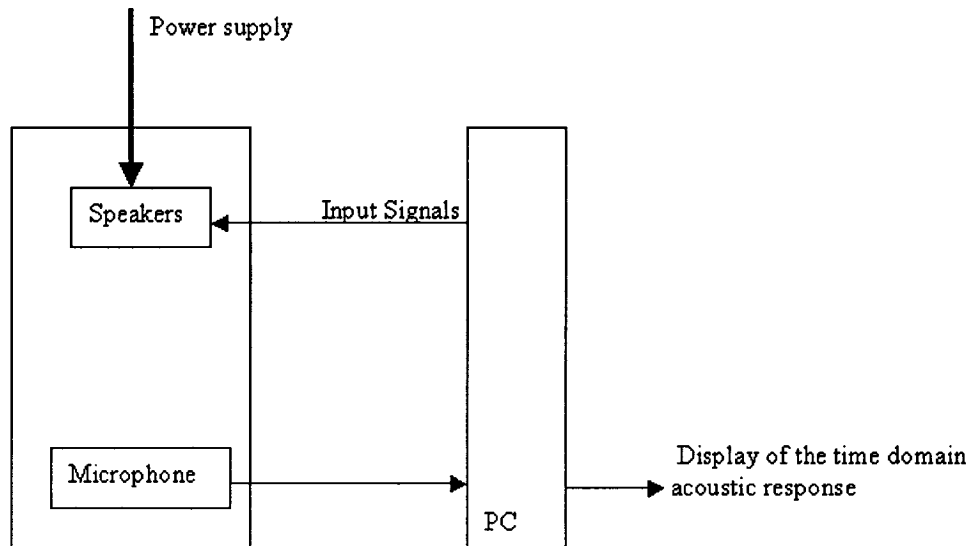


Figure 6-6 Experimental setup for room acoustics measurement

Fig.6-6 shows the experimental setup for room acoustics measurement. An omnidirectional speaker renders a sound file, shown in Fig.6-7. The experimental results will be compared with the simulation results to demonstrate the experiment efficiently. The previous input signals for simulation have long duration. The simulation for the previous signals is completed due to the large size of the simulated room. However, the room for the experimental study is smaller than the simulated room based on the image method on a digital computer. If we still use the signals with long duration, the computer will not be able to account for the high-level image sources. We have chosen this signals shown in Fig.6-7

[41] because its duration was satisfactory for this room. An omnidirectional microphone, which is connected to a computer, receives the signals using a sound card. The signals that the microphone receives are saved as the wave file. The signals with the wave file can be processed and displayed by Matlab.

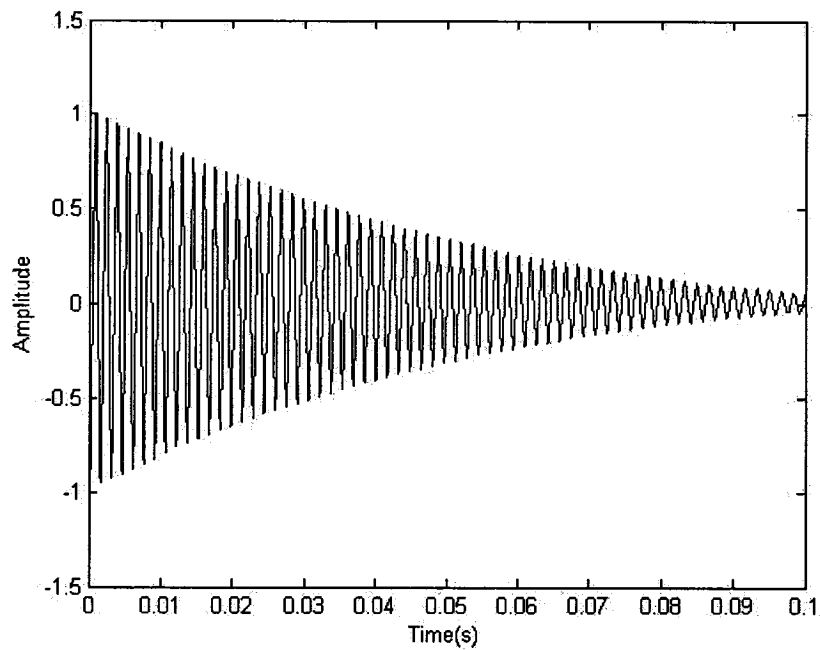


Figure 6-7 The input signals

Fig.6-7 shows a time-domain representation of the input signals. The time-domain graph gives the amplitudes of the individual samples. Except for time-domain representation there is the frequency-domain representation, which displays the frequencies the signals have. The frequency domain is very useful in digital signal processing, such as spectrum analyzers, and for choosing the sampling frequency. We implement the Fast Fourier Transform for the conversion of the input signals from the time-domain into the frequency-domain, shown in Fig.6-8.

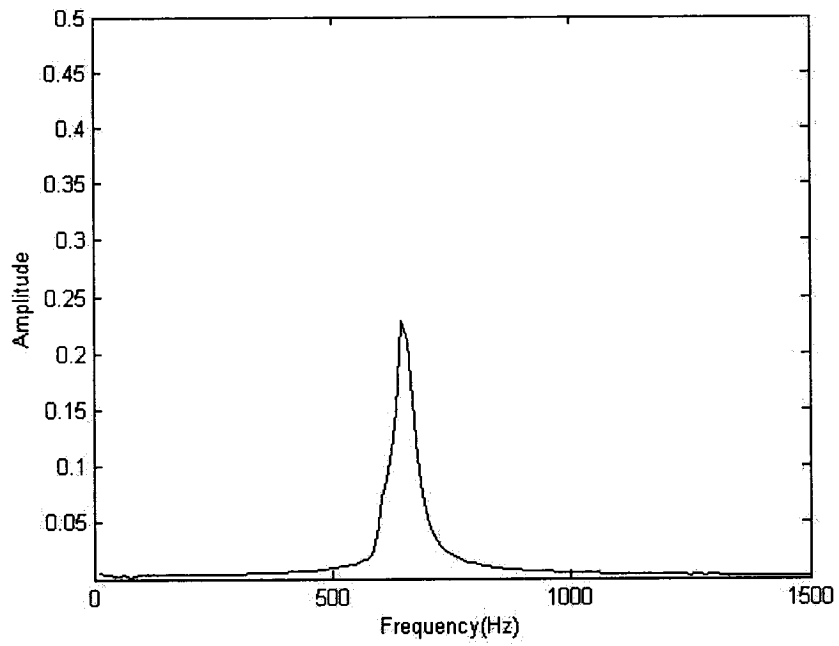


Figure 6-8 Frequency-domain representation of the input signals

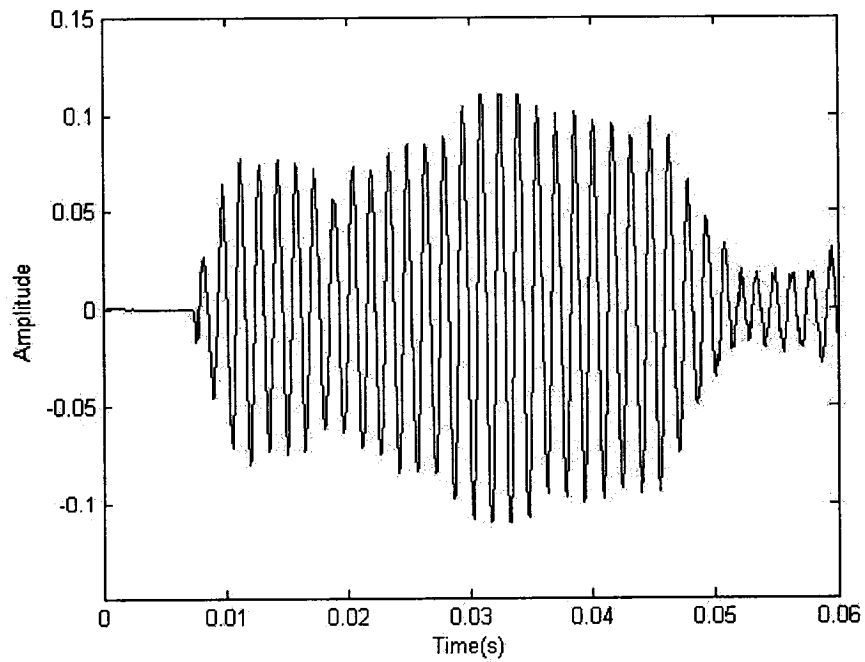


Figure 6-9 Experimental outputs of the signals from the microphone

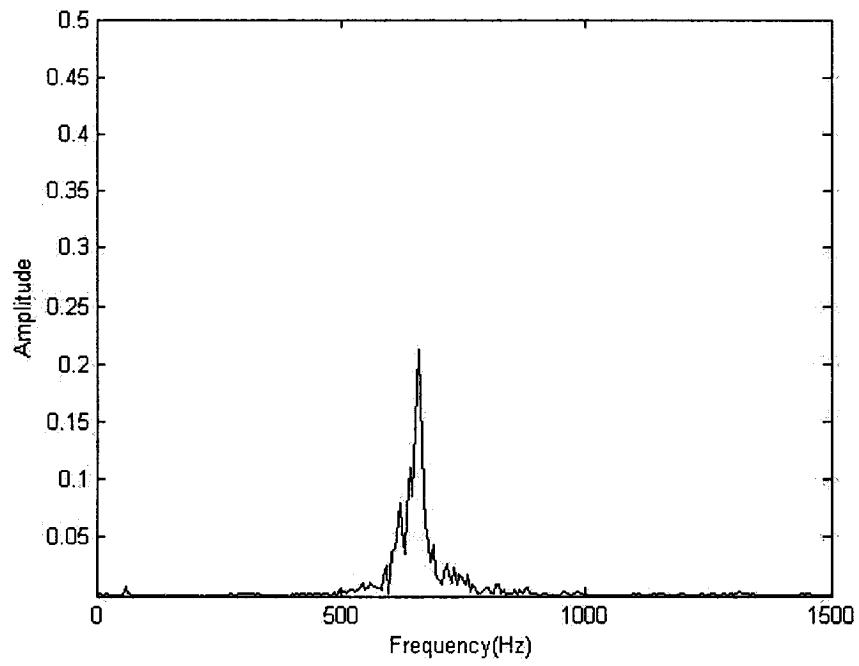


Figure 6-10 Frequency-domain representation of the output signals

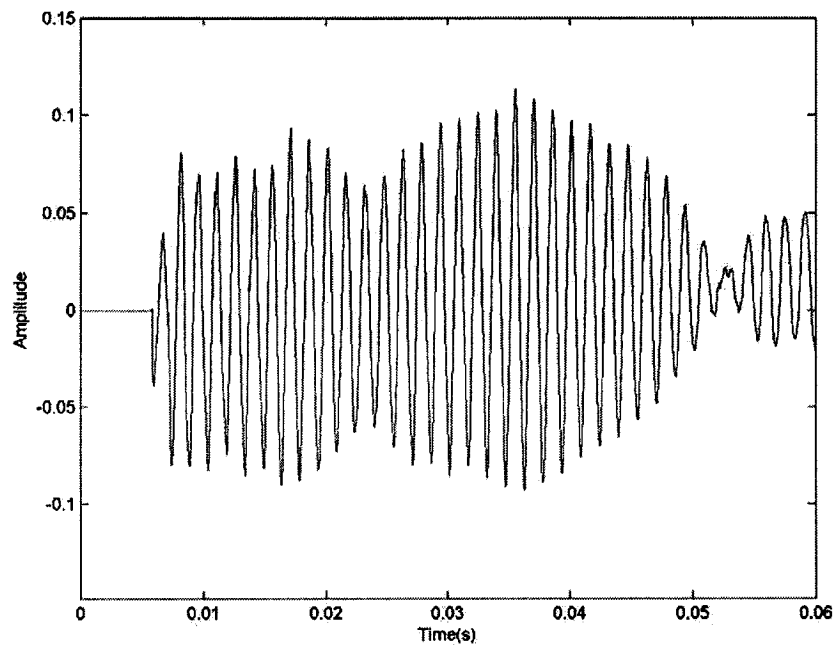


Figure 6-11 Simulation results at the microphone location

Fig.6-9 displays the signals the microphone receives. It can be seen that the experiment was originally carried out for as obvious in the power spectrum from Fig. 6-10. Fig. 6-11 shows the simulation results at the microphone location. The signals that are obtained by the experiment strongly resemble to the simulation results showed in Fig. 6-11.

In next experiments we consider this room with the significant external noise. The location of the speaker is at  $-1, 0.1, -0.5$ . The location of the microphone is at  $0.9, 0.4, -0.6$ . We apply the same input signals that are showed in Fig. 6-7. Fig. 6-12 displays the signals we received by the microphone. We can see that the signals contain the significant noise with frequency above 2200Hz, as shown in Fig. 6-13.

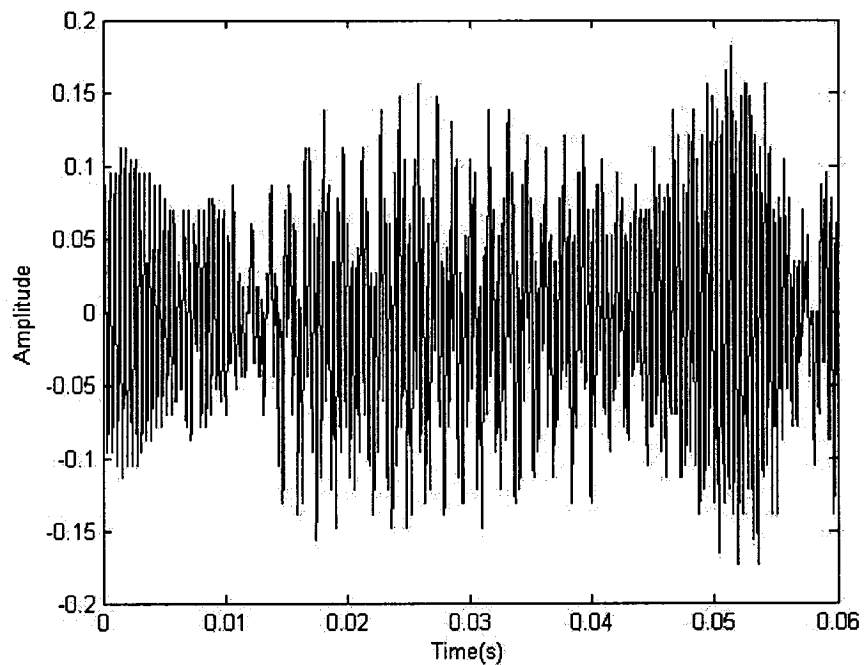


Figure 6-12 The output signals from the microphone with the significant noise

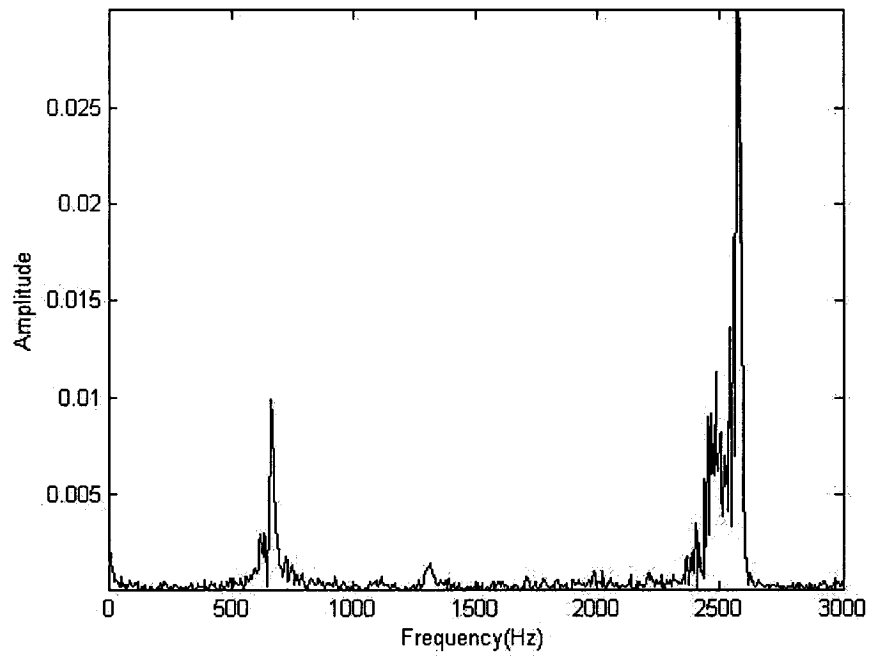


Figure 6-13 The frequency distribution of the output signals

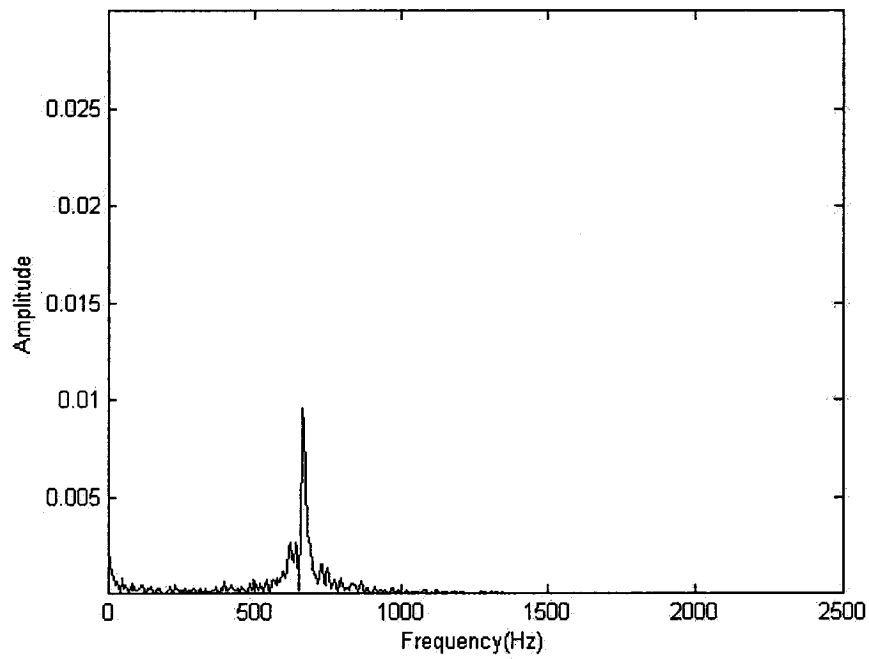


Figure 6-14 The frequency of the output signals after passing through the low pass filter with cut-off frequency 1500Hz

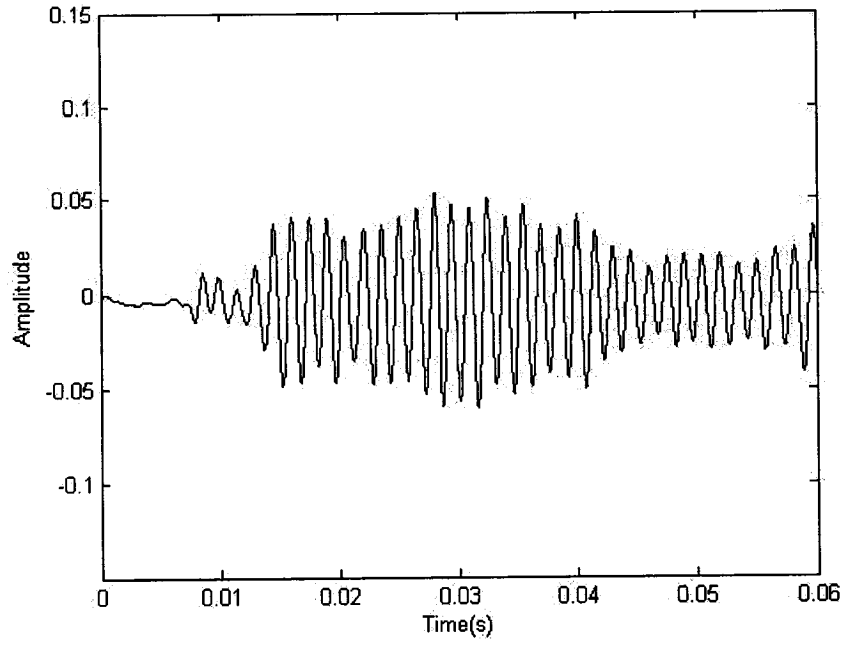


Figure 6-15 The output signals after passing through the low pass filter with the cut-off frequency 1500Hz

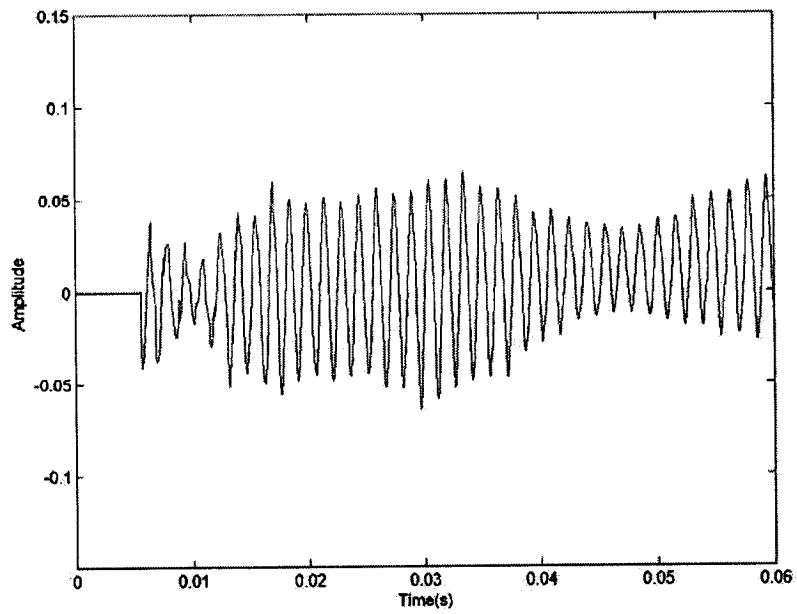


Figure 6-16 Simulation results for the results shown in Fig. 5-15

In order to remove the high frequency, a low pass filter from Matlab is applied. Fig. 6-15 shows the output signals after passing through a low pass filter with 1500Hz cut-off frequency. Fig. 6-14 shows the frequency-domain results for the output signals after passing through a low pass filter that has 1500Hz cut-off frequency, i.e. The signals shown in Fig. 6-15 don't include the signals whose frequencies are higher than 1500Hz. The simulation results using image method are displayed in Fig. 6-16. Compared with the signals illustrated in Fig. 6-16, the signals going through a 1500 low pass filter are very close to the simulation results.

So far, a rectangular room with no furniture has been used for the experimental study of room acoustics. The sound field in this room with the significant external noise has also been investigated. The results presented in this chapter proved that the design of the measurement system for room acoustics is proper compared with the simulation based on the image method.

## **Chapter 7**

### **Conclusions and recommendations for future work**

#### **7.1 Conclusion**

In this thesis eigenfrequencies were calculated to explore the sound field of a simple room using analytical method and FEMLAB software based on the finite element method. They confirm that it is convenient to simulate a sound field for the complex room geometry by FEMLAB software. FEMLAB software can displays the 3-D pressure distribution and it is very useful for room acoustics analysis. Even though these methods are limited to the low frequencies, the eigenfrequencies of the room are important for the sound study of the small listening room. As we mention in Chapter 3, calculation of the normal modes can predict the optimum dimensions. A cubic form is the worst form for room acoustics since each mode has triple emphasis. Choosing appropriate dimensions for the room can minimize the uneven sound coloration. If the dimensions of the room are difficult to change, the absorbing material is applied for reducing the sound coloration.

The image method for modeling the acoustic impulse response of a single source-receiver in a rectangular room was examined. This simulation model can be used for the prediction of the sound field in the room under different condition, such as different reflection coefficient. The experiment for room acoustic measurement is achieved and the

investigation of the sound field in the room was carried out for minimum noise and for significant noise. These prove that the experiment is the efficient method for measuring sound propagation in enclosure. This experiment system could be developed for evaluating the acoustic quality at different positions in the room.

## **7.2 Future work**

In the future research, the computational efficiency of the simulation model for more complicated phenomena of room acoustics in reality should be carried out. Several important factors, which violate assumption of geometrical room acoustics, have to be evaluated. Research topics to consider are as following:

- The simulation model is based on the assumption of geometrical room acoustics. The reflections from the surfaces of the room are simply specular reflections. Frequently the surfaces of the room aren't smooth and there are many irregularities whose dimensions aren't smaller than the wavelength, on them. Diffusion reflection may be considered which will make the prediction more efficient and accurate.
- The assumption that the sound source in the simulation model was an omnidirectional point source. In practice application, the directional characteristics of the sound source should be considered to get more realistic results.
- An algorithm, which is restricted to the rectangular room, computed the direct sound and early reflection in the simulation system, should be extended to more

complicated geometry, for example, several piece of furniture is considered in a polyhedral room.

- The experimental setup, based on xPC system may be applied for room acoustics measurement.

## Reference

- [1] Allan D. Pierce, *Acoustics: An Introduction to Its Physical Principles and Applications*. McGraw-Hill Book Company, 1981
- [2] Daniel R. Raichel, *The Science and Applications of Acoustics*. Springer-Verlag New York, Inc, 2000
- [3] Leo L. Beranek, *Concert Halls and Opera Houses: music, acoustics, and architecture*. Second Edition. Springer-Verlag New York, Inc, 2004
- [4] Heinrich Kuttruff, *Room Acoustics*. Third Edition, 1991. Elsevier Applied Science, London and New York
- [5] R. Walker, Acoustic modeling-approximations to the real world. *BBC Research & Development White Paper 005*
- [6] D.G.Crighton, A.P. Dowling, J.E.Ffowcs Williams, M.Heckl and F.G.Leppington, *Modern Methods in Analytical Acoustics*. Springer-Verlag, 1992
- [7] Malcolm J, Crocker, *Handbook of Acoustics*. John Wiley & Sons, Inc, 1998
- [8] A. Pietrzyk, Computer modeling of the sound field in small rooms. *Proc. AES 15th Int. Conf. on Audio, Acoustics & Small Spaces*, pages 24–31, Denmark, Nov. 1998.
- [9] U. P. Svensson and U. R. Kristiansen, Computational modelling and simulation of acoustic spaces. *The Proc. of the AES 22nd International Conference*, pages 11–30. Audio Engineering Society, Inc., June 2002.
- [10] Xuejun Xue, Xiang Yan, Xue Bai, The computer assistance application for architecture acoustics. <http://www.arch-world.cn/article/article.asp?sn=1602-20051206-0001>.
- [11] Andrzej, Kulowski, Algorithmic Representation of the Ray Tracing Technique. *Applied Acoustics* 18 (1985) 449-469.

- [12] A.Krokstad, S.Strom and S.Sorsdal, Calculating the acoustical room response by the use of a ray tracing technique. *J.Sound Vib.* 8 (1968), 118-125.
- [13] J.B.Allen and D.A. Berkley, Image method for efficiently simulating small-room acoustics. *J.Acoust.Soc.Am.* 65(4), 943-950, 1979
- [14] B.M. Gibbs and D.K. Jones, A Simple Image Method for Calculating the Distribution of Sound Pressure Levels within an Enclosure. *Acustica* 26,24-32 (1972)
- [15] Heewon Lee and Byung-Ho Lee, An Efficient Algorithm for the Image Model Technique. *Applied Acoustics* 24(1988) 87-115
- [16] A.Kulowski, Error investigation for the ray tracing technique. *Applied Acoustics* 15 (1982), 263-274.
- [17] H.Lehnert, Systematic errors of the ray-tracing algorithm. *Applied Acoustics.* 38(1993), 207-221.
- [18] Michael Vorlander, Simulation of the transient and steady-state sound propagation in rooms using a new combined ray-tracing/image-source algorithm. *J.Acoust.Soc.Am.* 86 (1989), 172-178.
- [19] A.Krokstad, S.Strom and S.Sorsdal, Fifteen Years' Experience with Computerized Ray tracing. *Applied Acoustics* 16 (1983) 201-312.
- [20] J. Kir szenstein, An Image Source Computer Model for Room Acoustics Analysis and Electroacoustic Simulation. *Applied Acoustics* 17 (1984) 275-290
- [21] Ramari Duraiswami, Nail A. Gumeroy, Dmitry N. Zotkin, Larry S. Davis, Efficient Evaluation of Reverberant Sound Fields. *IEEE Workshop on Application of Signal Processing to Audio and Acoustics* 2001.
- [22] Dr.Y.W.Lam, Geometrical Room Acoustics. University of Salford.  
<http://www.acoustics.salford.ac.uk>

- [23] M. Barron and C.B.Chinoy, 1:50 scale acoustic models for objective testing of auditoria. *Applied Acoustics*. 12 (1979), 361-375.
- [24] M. Kleiner, R. Orłowski and J. Kirszenstein, A comparison between results from a physical scale model and a computer image source model for architectural acoustics. *Applied Acoustics*. 38 (1993), 245-265.
- [25] R. Pompoli, A. Farina , P. Fausti, The acoustics of the ‘NUOVO TEATRO COMUNALE' in Cagliari. *International IOA Conference "Opera and Concert Hall Acoustics"*, London Gatwick, 10-12 February 1995.
- [26] Knudson, V.O, Absorption of sound in air, in oxygen and nitrogen-Effects of humidity and temperature. *J.Acoust.Soc.Am.* 3(1933), 112-121.
- [27] L.E.Kinsler et al, *Fundamentals of Acoustics*. J.Wiley, 2000
- [28] Leo L. Beranek, *Noise and Vibration Control Engineering: principles and application*. John Wiley & Sons Inc,1992
- [29] Leo L. Beranek, *Acoustics*. The American Institute of Physics, Inc,1986
- [30] C.L.S.Gilford, The acoustic design of talk studio and listening rooms. *J.Audio. Eng. Soc.* 27 (1979), 17-31.
- [31] M M Londen, Dimension ratios of rectangular rooms with good distribution of eigentone. *Acustica*. 24(1971), 101-104.
- [32] R. Walker, Optimum Dimension Ratios for Small Rooms. *100th Convention of the AES*. (5/1996).
- [33] R.C.Stanley, *Light and Sound for Engineers*. Hard Publishing Company,Inc, 1968
- [34] Ditten, Richard, *Modern geometrical optics*. Wiley, 1998.
- [35] L.H.Schaudinischeky, *Sound, Man and Building*. Applied Science Publishers LTD. 1976

- [36] Lawrence J. Ziomek, *Fundamentals of Acoustic Field Theory and Space-Time Signal Processing*. CRC Press, 1995
- [37] Eugen Skudrzyk, *The Foundations of Acoustics: Basic Mathematics and Basic Acoustics*. Springer-Verlag, New York. 1968.
- [38] Mitra, Sanjit Kumar, *Digital signal processing*. McGraw-Hill, 2001
- [39] D. Neculescu, *Mechatronics*. Prentice Hall, 2002
- [40] Craig Marven and Gillian Ewers, *A simple Approach to Digital Signal Processing*. John Wiley & Sons, Inc. 1996
- [41] <http://freesound.iaa.upf.edu/samplesViewRandom.php>
- [42] J.M. Blackledge, *Quantitative Coherent Imaging: Theory, methods and some applications*. Academic Press, 1989
- [43] FEMLAB 3 Modeling Guide, 2004.
- [44] FEMLAB 3 Model Library, 2004.

## Appendix: Simulation Codes in Matlab

```
function [X_in_Y,X,Y]=xy_creat(r)

%a,b,c - length, width, and height of the single room
%R - radius of the ball
%m,n,p - the coordinates(x,y,z) of the source point in the room

global x_max %the maximun numbers of room along x axis
global y_max %the maximun numbers of room along y axis
global z_max %the maximun numbers of room along z axis
global a
global b
global c
global m
global n
global p

X_in_Y=zeros(1,y_max);
X=zeros(y_max,x_max);
Y=zeros(y_max,x_max);

% calculation x coordinate and y coordinate of every image source point
for i1=0:(y_max-1)/2
    tt1=((y_max-1)/2+1)+i1;
    tt2=((y_max-1)/2+1)-i1;
    j1=0;
    jj=0;
    r1=sqrt(r^2-(i1*b)^2);
    if r1>0
        while j1<1000
            t1=a/2+a*j1;
            if (t1<r1)
                tt3=((x_max-1)/2+1)+j1;
                tt4=((x_max-1)/2+1)-j1;
                if j1==0
                    X(tt1,tt3)=m;
                    X(tt2,tt3)=m;
                end
                if mod(j1,2)==1
                    X(tt1,tt3)=j1*a-m;
                    X(tt1,tt4)=-j1*a-m;
                    X(tt2,tt3)=j1*a-m;
```

```

        X(tt2,tt4)=-j1*a-m;
    end
    if mod(j1,2)==0
        X(tt1,tt3)=j1*a+m;
        X(tt1,tt4)=-j1*a+m;
        X(tt2,tt3)=j1*a+m;
        X(tt2,tt4)=-j1*a+m;
    end
    if i1==0
        Y(tt1,tt3)=n;
        Y(tt2,tt3)=n;
        Y(tt1,tt4)=n;
        Y(tt2,tt4)=n;
    end
    if mod(i1,2)==1
        Y(tt1,tt3)=i1*b-n;
        Y(tt1,tt4)=i1*b-n;
        Y(tt2,tt3)=-i1*b-n;
        Y(tt2,tt4)=-i1*b-n;
    end
    if mod(i1,2)==0
        Y(tt1,tt3)=i1*b+n;
        Y(tt1,tt4)=i1*b+n;
        Y(tt2,tt3)=-i1*b+n;
        Y(tt2,tt4)=-i1*b+n;
    end
    end

    j1=j1+1;
    jj=j1;

else
    j1=1001;
end
end
X_in_Y(tt1)=2*jj+1;
X_in_Y(tt2)=2*jj+1;

end
end

```

```
function [X_in_Y_in_Z,room_array_x,room_array_y,num_level_Z]=room_creat
```

```
%a,b,c - length, width, and height of the single room
```

```
%R - radius of the ball
```

```
%m,n,p - the coordinates(x,y,z) of the source point in the room
```

```
global x_max %the maximum numbers of room along x axis
```

```
global y_max %the maximum numbers of room along y axis
```

```
global z_max %the maximum numbers of room along z axis
```

```
global a
```

```
global b
```

```
global c
```

```
global m
```

```
global n
```

```
global p
```

```
% initial conditions
```

```
a=40.23;
```

```
b=13.41;
```

```
c=20.70;
```

```
R=30; %assuming t=0.1s,R=c*t,c=343m/s(sound propagation in the air)
```

```
m=-1.2 % m=-1;
```

```
n=0.14 % n=-1;
```

```
p=-0.5 % p=-1;
```

```
% calculation the maximum numbers of room along x axis.
```

```
i=0;
```

```
while (i<1000)
```

```
    t1=a/2+a*i;
```

```
    if t1<R
```

```
        i=i+1;
```

```
    else
```

```
        x_max=2*i+1;
```

```
        i=1001;
```

```
    end
```

```
end
```

```
% calculation the maximum number of rooms at y axis.
```

```
i=0;
```

```
while (i<1000)
```

```
    t1=b/2+b*i;
```

```
    if t1<R
```

```
        i=i+1;
```

```
    else
```

```
        y_max=2*i+1;
```

```

    i=1001;
end
end

% calculation the maximun number of rooms at z axis.
i=0;
while (i<1000)
    t1=c/2+c*i;
    if t1<R
        i=i+1;
    else
        z_max=2*i+1;
        i=1001;
    end
end
end
% room_array_x is 3-D array including x coordinate of every image source
% room_array_y is 3-D array including y coordinate of every image source
% X_in_Y_in_Z is 2-D array including the numbers of the room along x axis
% in the relative y position
% num_level_array is 1-D array including z coordinate of every image source
room_array_x=zeros(y_max,x_max,z_max);
room_array_y=zeros(y_max,x_max,z_max);
X_in_Y_in_Z=zeros(z_max,y_max);
num_level_Z=zeros(1,z_max);

% calculation z coordinate of every image source
for i=0:(z_max-1)/2
    if R>(c/2)+i*c
        r=sqrt(R^2-((c/2)+i*c)^2);
        t1=((z_max-1)/2+1)+i;
        t2=((z_max-1)/2+1)-i;
        if i==0
            num_level_Z(t1)=p;
        end
        if mod(i,2)==1
            num_level_Z(t1)=i*c-p;
            num_level_Z(t2)=-i*c-p;
        end
        if mod(i,2)==0
            num_level_Z(t1)=i*c+p;
            num_level_Z(t2)=-i*c+p;
        end
        %get 3-D coordinates of every image source
        [X_in_Y_in_Z(t1,:),room_array_x(:,t1),room_array_y(:,t1)]=xy_creat(r);
        [X_in_Y_in_Z(t2,:),room_array_x(:,t2),room_array_y(:,t2)]=xy_creat(r);
    else
        r=0;
    end
end

```

```

    end
end

% calculation the distance between two points in 3-D environment
% P1,P2 are 1x3 vectors
function d=dist_3d(P1,P2)

d=sqrt((P1(1)-P2(1))^2+(P1(2)-P2(2))^2+(P1(3)-P2(3))^2);

% the simple impulse response of the room, the input of the source is
% a pulse whose amplitude is one, the room has rigid surfaces
function Result_pulse1

global x_max
global y_max
global z_max

X=zeros(y_max,x_max,z_max);
Y=zeros(y_max,x_max,z_max);
Z=zeros(1,z_max);

location=[5,2,-5];

[m,X,Y,Z]=room_creat;

distance=zeros(1,x_max*y_max*z_max);
t=zeros(1,x_max*y_max*z_max);

num=1;
for i=1:z_max
    for j=1:y_max
        for k=1:x_max
            if X(j,k,i)==0&Y(j,k,i)==0

                else
                    current=[X(j,k,i),Y(j,k,i),Z(i)];
                    distance(num)=dist_3d(location,current);
                    d(num)=1/(4*pi*distance(num));
                    t(num)=distance(num)/343;
                    plot([t(num),t(num)],[0,d(num)],'-')
                    xlabel('Time(s)')
                    ylabel('Amplitude')
                    hold on
                    num=num+1;
                end
            end
        end
    end
end

```

```

    end
  end
end

```

% The simple impulse response of the room, the input of the source is  
 % a pulse whose amplitude is one, the room has nonrigid surfaces

**function Result\_pulse2**

```

global x_max
global y_max
global z_max

```

```

X=zeros(y_max,x_max,z_max);
Y=zeros(y_max,x_max,z_max);
Z=zeros(1,z_max);

```

```

location=[5,2,-5];

```

```

[m,X,Y,Z]=room_creat;

```

```

distance=zeros(1,x_max*y_max*z_max);
t=zeros(1, x_max*y_max*z_max);

```

```

num=1;
Q11=0.7
Q12=0.7
Q21=0.9
Q22=0.9
Q31=0.9
Q32=0.9
for i=1:z_max
  for j=1:y_max
    for k=1:x_max
      if X(j,k,i)==0&Y(j,k,i)==0

        else

          i1=i-((z_max-1)/2+1);
          if mod(i1,2)==0
            q1=(Q11^abs(i1/2))*(Q12^abs(i1/2));
          else
            q1=(Q11^abs(i1/2-1))*(Q12^abs(i1/2+1));
          end

          j1=j-((y_max-1)/2+1);
          if mod(j1,2)==0

```

```

        q2=(Q21^abs(j1/2))*(Q22^abs(j1/2));
    else
        q2=(Q21^abs(j1/2-1))*(Q22^abs(j1/2+1));
    end

    k1=k-((x_max-1)/2+1);
    if mod(k1,2)==0
        q3=(Q31^abs(k1/2))*(Q32^abs(k1/2));
    else
        q3=(Q31^abs(k1/2-1))*(Q32^abs(k1/2+1));
    end

    current=[X(j,k,i),Y(j,k,i),Z(i)];
    distance(num)=dist_3d(location,current);
    d(num)=(q1*q2*q3)/(4*pi*distance(num));
    t(num)=distance(num)/343;
    plot([t(num),t(num)],[0,d(num)],'-')
    xlabel('Time(s)')
    ylabel('Amplitude')
    hold on
    num=num+1;

end
end
end
end

```

```

% a room of dimension by 40.23 by 13.41 by 20.70,the receiver is located in
% [5,2,-5]. Surfaces of the room are rigid surfaces. The source is a sine
% wave

```

### **function Result\_sinewave1**

```

global x_max
global y_max
global z_max

X=zeros(y_max,x_max,z_max);
Y=zeros(y_max,x_max,z_max);
Z=zeros(1,z_max);

location=[5,2,-5];

[m,X,Y,Z]=room_creat;

distance=zeros(1,3*max([x_max,y_max,z_max]));

```

```

t=zeros(1,3*max([x_max,y_max,z_max]));

num=1;
for i=1:z_max
    for j=1:y_max
        for k=1:x_max
            if X(j,k,i)==0&Y(j,k,i)==0

                else
                    current=[X(j,k,i),Y(j,k,i),Z(i)];
                    distance(num)=dist_3d(location,current);
                    D(num)=1/(4*pi*distance(num));
                    num=num+1;
                end
            end
        end
    end
end

max_d=0;
min_d=1000;
max_num=0;
min_num=0;
[a,b]=size(distance)
for i=1:b
    if distance(i)~=0;
        if min_d>distance(i)
            min_d=distance(i);
            min_num=i;
        end
        if max_d<distance(i)
            max_d=distance(i);
            max_num=i;
        end
    end
end
distance;
max_d
min_d

figure(1)
axis([0 0.4 -0.015 0.015])
xlabel('Time(s)')
ylabel('Amplitude')
hold on

```

```

%i=1;
y=0;
T=(min_d/343:0.0001:max_d/343+0.01);
[c,d]=size(T)
for i=1:d
    y=0;
    for j=1:b
        if distance(j)~=0
            if T(i)<=(distance(j)/343+0.01)&T(i)>=(distance(j)/343)
                y=y+sin(200*pi*(T(i)-distance(j)/343))*D(j);
            end
        end
    end
    plot([T(i),T(i)],[0,y],'-')
end

```

% a room of dimension by 40.23 by 13.41 by 20.70,the receiver is located in  
% [5,2,-5]. Surfaces of the room are nonrigid surfaces. The source is a sine  
% wave file.

#### **function Result\_sinewave2**

```

global x_max
global y_max
global z_max

X=zeros(y_max,x_max,z_max);
Y=zeros(y_max,x_max,z_max);
Z=zeros(1,z_max);

location=[5,2,-5];

[m,X,Y,Z]=room_creat;

distance=zeros(1,3*max([x_max,y_max,z_max]));
t=zeros(1,3*max([x_max,y_max,z_max]));

num=1;
Q11=0.7
Q12=0.7
Q21=0.9
Q22=0.9
Q31=0.9
Q32=0.9
for i=1:z_max

```

```

for j=1:y_max
  for k=1:x_max
    if X(j,k,i)==0&Y(j,k,i)==0

      else

        i1=i-((z_max-1)/2+1);
        if mod(i1,2)==0
          q1=(Q11^abs(i1/2))*(Q12^abs(i1/2));
        else
          q1=(Q11^abs(i1/2-1))*(Q12^abs(i1/2+1));
        end

        j1=j-((y_max-1)/2+1);
        if mod(j1,2)==0
          q2=(Q21^abs(j1/2))*(Q22^abs(j1/2));
        else
          q2=(Q21^abs(j1/2-1))*(Q22^abs(j1/2+1));
        end

        k1=k-((x_max-1)/2+1);
        if mod(k1,2)==0
          q3=(Q31^abs(k1/2))*(Q32^abs(k1/2));
        else
          q3=(Q31^abs(k1/2-1))*(Q32^abs(k1/2+1));
        end

        current=[X(j,k,i),Y(j,k,i),Z(i)];
        distance(num)=dist_3d(location,current);
        D(num)=(q1*q2*q3)/(4*pi*distance(num));
        num=num+1;

      end
    end
  end
end

max_d=0;
min_d=1000;
max_num=0;
min_num=0;
[a,b]=size(distance);
for i=1:b
  if distance(i)~=0;
    if min_d>distance(i)
      min_d=distance(i);
      min_num=i;
    end
  end
end

```

```

end
if max_d < distance(i)
    max_d = distance(i);
    max_num = i;
end
end
end
distance;
max_d;
min_d;

figure(1)
axis([0 0.4 -0.015 0.015])
xlabel('Time(s)')
ylabel('Amplitude')
hold on
y=0;
T=(min_d/343:0.0001:max_d/343+0.01);
[c,d]=size(T)
for i=1:d
    y=0;
    for j=1:b
        if distance(j)~=0
            if T(i)<=(distance(j)/343+0.01)&T(i)>=(distance(j)/343)
                y=y+sin(200*pi*(T(i)-distance(j)/343))*D(j);
            end
        end
    end
    plot([T(i),T(i)],[0,y],'-')
end
end

```

% a room of dimension by 40.23 by 13.41 by 20.70, the receiver is located in  
 % [5,2,-5]. Surfaces of the room are rigid surfaces. The source is a sound  
 % wave file.

### **function Result\_sound1**

```

global x_max
global y_max
global z_max

X=zeros(y_max,x_max,z_max);
Y=zeros(y_max,x_max,z_max);
Z=zeros(1,z_max);

```

```

location=[5,2,-5];

[m,X,Y,Z]=room_creat;

distance=zeros(1,3*max([x_max,y_max,z_max]));
t=zeros(1,3*max([x_max,y_max,z_max]));

num=1;
for i=1:z_max
    for j=1:y_max
        for k=1:x_max
            if X(j,k,i)==0&Y(j,k,i)==0

                else
                    current=[X(j,k,i),Y(j,k,i),Z(i)];
                    distance(num)=dist_3d(location,current);
                    num=num+1;
                end
            end
        end
    end
end

max_d=0;
min_d=1000;
max_num=0;
min_num=0;
[a,b]=size(distance)
for i=1:b
    if distance(i)~=0;
        if min_d>distance(i)
            min_d=distance(i);
            min_num=i;
        end
        if max_d<distance(i)
            max_d=distance(i);
            max_num=i;
        end
    end
end
end
max_d
min_d

[Y,Fs]=sound;

```

```

C=round(max_d*Fs/343);
D=C+length(Y);
E=zeros(b,D);
EE=zeros(1,D);
for i=1:b
    s(i)=round(distance(i)*Fs/343);
    G(i)=1/(4*pi*distance(i));
    for j=1:D
        if j<s(i)|j>s(i)+length(Y)-1
            E(i,j)=0;
        else
            E(i,j)=Y(j-s(i)+1);
        end
        EE(j)=EE(j)+G(i)*E(i,j);
    end
end
T=(1:D)/Fs;
figure(2)
plot(T,EE)
axis tight
xlabel('Time(s)')
ylabel('Amplitude')
wavwrite(EE,Fs,'beauty')

```

% a room of dimension by 40.23 by 13.41 by 20.70,the receiver is located in  
 % [5,2,-5]. Surfaces of the room are nonrigid surfaces. tha source is a sound  
 % wave file.

### **function Result\_sound2**

```

global x_max %the maximun numbers of room along x axis
global y_max %the maximun numbers of room along y axis
global z_max %the maximun numbers of room along z axis

```

```

X=zeros(y_max,x_max,z_max);
Y=zeros(y_max,x_max,z_max);
Z=zeros(1,z_max);

```

```

location=[5,2,-5] % the location of the receiver

```

```

[m,X,Y,Z]=room_creat;

```

```

distance=zeros(1,3*max([x_max,y_max,z_max]));
t=zeros(1,3*max([x_max,y_max,z_max]));

```

```

num=1;
Q11=0.7 % reflection coefficient from -z wall

```

```

Q12=0.7 % reflection coefficient from +z wall
Q21=0.9 % reflection coefficient from -y wall
Q22=0.9 % reflection coefficient from +y wall
Q31=0.9 % reflection coefficient from -x wall
Q32=0.9 % reflection coefficient from +x wall

% calculate the intensity of each image source
for i=1:z_max
    for j=1:y_max
        for k=1:x_max
            if X(j,k,i)==0&Y(j,k,i)==0

                else

                    i1=i-((z_max-1)/2+1);
                    if mod(i1,2)==0
                        q1=(Q11^abs(i1/2))*(Q12^abs(i1/2));
                    else
                        q1=(Q11^abs(i1/2-1))*(Q12^abs(i1/2+1));
                    end

                    j1=j-((y_max-1)/2+1);
                    if mod(j1,2)==0
                        q2=(Q21^abs(j1/2))*(Q22^abs(j1/2));
                    else
                        q2=(Q21^abs(j1/2-1))*(Q22^abs(j1/2+1));
                    end

                    k1=k-((x_max-1)/2+1);
                    if mod(k1,2)==0
                        q3=(Q31^abs(k1/2))*(Q32^abs(k1/2));
                    else
                        q3=(Q31^abs(k1/2-1))*(Q32^abs(k1/2+1));
                    end

                    current=[X(j,k,i),Y(j,k,i),Z(i)];
                    distance(num)=dist_3d(location,current);
                    O(num)=(q1*q2*q3)/(4*pi*distance(num));
                    num=num+1;

                end
            end
        end
    end

max_d=0;
min_d=1000;

```

```

max_num=0;
min_num=0;
[a,b]=size(distance);
for i=1:b
    if distance(i)~=0;
        if min_d>distance(i)
            min_d=distance(i);
            min_num=i;
        end
        if max_d<distance(i)
            max_d=distance(i);
            max_num=i;
        end
    end
end
distance;
max_d,
min_d,

[Y,Fs]=sound;    %Y is the sound data and Fs is the samlpe frequency of the current
sound
% calculate all the responses from every image source and get the sum response for this
room
C=round(max_d*Fs/343);
D=C+length(Y);
E=zeros(b,D);
EE=zeros(1,D);
for i=1:b
    s(i)=round(distance(i)*Fs/343);
    for j=1:D
        if j<s(i)|j>s(i)+length(Y)-1
            E(i,j)=0;
        else
            E(i,j)=O(i)*Y(j-s(i)+1);
        end
        EE(j)=EE(j)+E(i,j);
    end
end
T=(1:D)/Fs;
figure(2)
plot(T,EE)
axis ([0 0.8 -0.015 0.015])
xlabel('Time(s)')
ylabel('Amplitude')
wavwrite(EE,Fs,'beauty1') % save the data to the sound file(beauty1.wav)

```

```

% sound in anechoic room
function source
[y,Fs]=wavread('original sound');
y % taking a sound file as a source,y is sound data, Fs is sample frequency.
m=-1;
n=-1;
p=-1;
x=5;
y1=2;
z=-5;
D=sqrt((x-m)^2+(y1-n)^2+(z-p)^2);
T=round(D*Fs/343);
T1=length(y)+T
t=(1:T1)/Fs
Y=zeros(1,T1)
for a=1:T1
    if a<T
        Y(a)=0;
    else
        Y(a)=y(a-T+1)/(4*pi*D);
    end
end
end
Y
plot(t,Y)
axis tight
xlabel('Time(s)')
ylabel('Amplitude')
wavwrite (Y,Fs,'sound without room')

```

%frequency-domain representation

**function [y,Fs]=analyze()**

```

[y,Fs] = wavread('3.wav'); % y is sound data, Fs is sample frequency.
t = (1:length(y))/Fs; % time
figure(1);
plot(t,y);
axis tight

```

```

N = 2^12; % number of points to analyze
c = fft(y(1:N))/N; % compute fft of sound data
p = 2*abs( c(2:N/2)); % compute power at each frequency
f = (1:N/2-1)*Fs/N; % frequency corresponding to p

```

```

figure(2)
semilogy(f,p)
plot(f,p)
axis([0 1000 10^-4 0.5])

```

**function[y,Fs]=lowpassfilter()**

```

[y,Fs] = wavread('file name.wav'); % y is sound data, Fs is sample frequency.
t = (1:length(y))/Fs; % time
figure(1);
plot(t,y);
axis ([0 0.06 -0.2 0.2])
xlabel('Time(s)')
ylabel('Amplitude')

N = 2^12;
c = fft(y(1:N))/N;
p = 2*abs( c(2:N/2));
f = (1:N/2-1)*Fs/N;

```

```

figure(2)
semilogy(f,p)
plot(f,p)
axis([0 3000 10^-4 0.03])
xlabel('Frequency(Hz)')
ylabel('Amplitude')

```

```

[b,a]=butter(6,0.078,'low'); %cutoff frequency is 1500Hz
y1p=filter(b,a,y)
figure(3)
plot(t,y1p);
axis ([0 0.06 -0.15 0.15])
xlabel('Time(s)')
ylabel('Amplitude')
N = 2^12;
c1 = fft(y1p(1:N))/N;
p1= 2*abs( c1(2:N/2));
f1= (1:N/2-1)*Fs/N;

```

```

figure(4)
semilogy(f1,p1)
plot(f1,p1)
axis([0 2500 10^-4 0.03])
xlabel('Frequency(Hz)')
ylabel('Amplitude')

```